J Eng Math (2009) 63:355–399
DOI 10.1007/s10665-008-9241-3

Large-degree asymptotics and exponential asymptotics for Fourier, Chebyshev and Hermite coefficients and Fourier transforms

John P. Boyd

Received: 16 June 2007 / Accepted: 1 August 2008 / Published online: 4 September 2008

Abstract When a function is expanded as
$f(x) \approx \sum_{n=0}^{N-1} a_n \phi_n(x)$
for some set of basis functions $\phi_j(x)$, its spectral coefficients a_n generally have an asymptotic approximation, as $n \to \infty$, in the form of an inverse power series plus terms that decrease exponentially with n. If $f(x)$ is analytic on the expansion interval, then all the coefficients of the inverse power series are zero and the problem becomes one of "beyond-all-orders" or "exponential" asymptotics. The method of steepest descent for integrals and other complex-path integration techniques can successfully connect the exponentially small behavior of the spectral coefficients to the singularities of $f(x)$ off the expansion interval. Many examples are given in both one and two dimensions.

Keywords Asymptotic approximation · Chebyshev polynomials · exponential asymptotics · Fourier series · steepest descent

1 Introduction

When a function is approximated by a spectral series, practical success hinges on how rapidly the coefficients a_n decrease with n. ϕ_n may denote the sines and cosines or complex exponentials of a Fourier series, Chebyshev or other orthogonal polynomials, rational Chebyshev functions and a variety of even more exotic possibilities.

The literature offers thousands of theorems on the convergence or divergence of various series under various conditions, but to the applied mathematician or engineer, the binary "converge/diverge" question is as useless as the answer to "Will the Sun die?" Instead, the fundamental practical question is: Does a given error tolerance ϵ require $N = 10$ or $N = 10{,}000{,}000$ where N is the number of terms in the spectral series? In the former case, a workstation will yield an answer even for three dimensions in a fraction of a second whereas the latter may be as unattainable, even on a petaflop computer, as the north pole of Pluto.

J. P. Boyd (✉)
Department of Atmospheric, Oceanic and Space Science, University of Michigan,
2455 Hayward Avenue, Ann Arbor, MI 48109-2143, USA
e-mail: jpboyd@umich.edu

The asymptotic theory of spectral coefficients is therefore important. One essential subtopic is: why does a certain basis work well or badly for a particular problem? What can be done to remedy slow convergence by modifying the numerical problem or choice of basis functions? Another goal is to estimate *a priori* the feasibility of a calculation.

There are several fundamental principles to the asymptotic theory of spectral coefficients. The first is Darboux's Principle: the asymptotic rate of convergence of a spectral series—Fourier, Chebyshev polynomial, Taylor series—is controlled by the *singularities* of $f(x)$ in the complex x-plane. (By singularities we mean discontinuities, poles, fractional powers, logarithms and other branch points: all points of non-analyticity in the sense of complex variable theory). Each singularity contributes a term or terms to the asymptotic approximation of a_n as $n \to \infty$; the leading order in a_n is controlled by the "worst" singularity, which is whichever discontinuity or pole or branch point contributes the *slowest-decaying* term to a_n.

The second key idea is the Model Function Method. All functions with simple poles at the same location with the same residue as the "worst singularity" will have the same leading-order asymptotic spectral coefficients. Consequently, one can learn much about the performance of spectral methods on real problems by studying the convergence for simple model functions that have the anticipated singularities.

The third important theme is that the classical tools of asymptotics for integrals—repeated integration-by-parts, steepest descent, the calculus of residues and so on—can be effectively applied to the usual orthogonality integrals

$$a_n = \int f(x)\, \phi_n(x) w(x) \mathrm{d}x, \tag{1}$$

where $w(x)$ is the weight function associated with the basis set ϕ_n. Often, much can be learned merely by looking up the asymptotic expansions of classical transcendentals in a handbook as illustrated below.

There are several goals or problems in spectral coefficient asymptotics. The first is to calculate *bounds* of the form

$$|a_n| \le p n^{-k} \quad \forall n \quad \text{or} \quad |a_n| \le p s(n) \exp(-\mu n) \quad \forall n, \tag{2}$$

where k in the first, power-law bound is the "algebraic index of convergence", μ in the second, exponential bound is the "asymptotic rate of geometric convergence" as in [1], p is a positive constant and $s(n)$ is a function that varies more slowly than the exponential. The second goal is to replace the inequalities by *complete asymptotics* with explicit formulas for p, k, μ and $s(n)$. The third goal is the *inverse* problem of identifying the convergence-limiting singularities from the asymptotic form of the spectral coefficients. We shall discuss all three types of problems in what follows.

Generically, the asymptotic approximation to a_n as $n \to \infty$ consists of two parts. The first is a series of inverse powers of n, or of other functions that decrease *algebraically* with n. The second is a collection of terms that are *exponentially small* in n. A concrete example may make the pattern clearer.

The complex-valued Fourier series on the interval $x \in [a, b]$ may be written, introducing the auxiliary parameter $\sigma \equiv 2\pi/(b-a)$

$$f(x) = \sum_{n=-\infty}^{\infty} c_n \exp(\mathrm{i} n \sigma x), \tag{3}$$

$$c_n = \frac{1}{b-a} \int_a^b f(x)\ \exp(-\mathrm{i} n \sigma x)\ \mathrm{d}x. \tag{4}$$

The usual cosine and sine coefficients are related to the complex coefficients (assuming $f(y)$ to be real-valued) via

$$a_n = 2\mathfrak{Re}(c_n); \qquad b_n = -2\mathfrak{Im} c_n \qquad \forall n > 0. \tag{5}$$

One can derive the inverse power series in n by the humble device of integration-by-parts, repeatedly integrating the basis function and differentiating $f(x)$, a strategy that works equally well for most other kinds of spectral series as illustrated later. For arbitrary J (assuming sufficient differentiability of $f(x)$):

$$c_n = \frac{\exp(-\mathrm{i}n\sigma a)}{b-a} \sum_{j=0}^{J} (-1)^j \left(\frac{\mathrm{i}}{n\sigma}\right)^{j+1} \left\{ f^{(j)}(b) - f^{(j)}(a) \right\} \tag{6}$$

$$+ \frac{1}{b-a} \left(-\frac{\mathrm{i}}{n\sigma}\right)^{J+1} \int_a^b f^{(J+1)}(x)\ \exp(-\mathrm{i}n\sigma x)\,\mathrm{d}x. \tag{7}$$

This formula is *exact*. The Fourier Asymptotic Coefficient Expansion (FACE) at J-th order, as named by Lyness [2,3], results from neglecting the integral.

When any of the terms in the inverse power series for a_n is nonzero, the spectral series for $f(x)$ is said to be "algebraically convergent". If $a_n \sim O(1/n^k)$ as $n \to \infty$, then k is said to be the "algebraic convergence order".

Algebraically convergent series are important in applications, as explained below. However, if $f(x)$ is free of singularities on the expansion interval (which requires $f(x) = f(x+P)$ for Fourier series where P is the period), then all coefficients in the inverse power series are *identically zero* and a_n decays *exponentially fast* as $n \to \infty$ [2,4].

In recent years, there has been much progress in what is variously called "beyond-all-orders asymptotics" (in the sense of calculating corrections smaller than any finite inverse power of n) or "exponential asymptotics" (because such corrections decay exponentially with n) [5–17]. For functions that are analytic on the expansion interval, asymptotic spectral coefficient analysis is always "beyond-all-orders".

A Fourier example with "beyond-all-orders" coefficients is

$$\lambda(x;\, p) \equiv \frac{(1-p^2)}{(1+p^2) - 2p\ \cos(x)} \tag{8}$$

$$= 1\ +\ 2 \sum_{n=1}^{\infty} \exp(-na)\ \cos(nx) \tag{9}$$

$$= 2\,a \sum_{m=-\infty}^{\infty} \frac{1}{\left(a^2\ +\ (x\ -\ 2\pi m)^2\right)}, \tag{10}$$

where $a \equiv -\ \log(p)\ \leftrightarrow\ p = \exp(-a)$. The partial-fraction expansion in the last line shows explicitly that this function is singular in the rectangle $\mathfrak{Re}(x) \in [-\pi, \pi]$, $\mathfrak{Im}(x) =$ anything, only through simple poles at $x = \pm \mathrm{i}a$ along the imaginary axis. ($f(x)$ is also singular at the images of these two poles under the periodicity shift, $x \to x + 2\pi m$ where m is an arbitrary integer.)

It is not an accident that the coefficients fall as $\exp(-n\mu)$ where $\mu = a$ is the imaginary part of the location of the singularity nearest the real axis; for Fourier series, the "asymptotic rate of convergence" μ is *always* the absolute value of the imaginary part of the singularity of $f(x)$ which is nearest the real axis.

In the remainder of this article, we shall show how broad assertions like this about the rate of convergence can be justified by asymptotic and exponential asymptotic approximations.

2 Connections between basis functions

Most of the asymptotic methods described here are broadly applicable to many species of basis functions, and not just one or two, because there are in fact close relationships between most of the basis sets used in spectral methods. For approximating a non-periodic $f(x)$ on a finite interval, Chebyshev polynomials are best. However, these are really just a cosine series in disguise where the "disguise" is a change of coordinates because of the identity

$$T_n(\cos(t)) \equiv \cos(nt) \qquad n = 0, 1, 2, \ldots\ \forall t. \tag{11}$$

Because of this, the theory of the asymptotic coefficients of Chebyshev series is almost the same as for Fourier series; often the best way to analyze the Chebyshev coefficient integral is to rewrite it as a Fourier integral:

$$a_n = \frac{2}{c_n \pi} \int_{-1}^{1} f(x) \frac{\mathrm{d}x}{\sqrt{1-x^2}} = \frac{2}{c_n\,\pi} \int_0^{\pi} f(\cos(t))\ \cos(nt)\mathrm{d}t, \tag{12}$$

where $c_0 = 2$ and $c_n = 1$ for all $n > 0$. The "almost" qualifier arises because the mapping $x = \cos(t)$ is *singular* at the endpoints $x = \pm 1$. A special analysis is needed for endpoint singularities and in fact Chebyshev series converge much faster when a given type of singularity is at the endpoints than when the same singularity is on the interior of the interval $x \in [-1, 1]$.

Similarly, the rational Chebyshev functions $TB_n(x; L)$, which are a good basis for $x \in [-\infty, \infty]$, are defined by

$$TB_n(L\cot(t); L) \equiv \cos(nt). \tag{13}$$

These were introduced (implicitly) by Grosch and Orszag [18]; their asymptotic coefficients were analyzed by Boyd [19,20]. Closely-related functions [21] were introduced by Christov [22–28].

Boyd introduced two different basis sets for the semi-infinite domain, $x \in [0, \infty]$

$$TL_n(x) \equiv \cos\left[2n \operatorname{arccot}\left(\sqrt{\frac{x}{L}}\right)\right], \tag{14}$$

$$TM_n(x; L) \equiv \cos(nt(x)), \qquad x = L\cot(t/2)\,\cos(t/2), \qquad t \in [0, \pi]. \tag{15}$$

The *TL* functions are studied in [29]. The *TM* functions perform better in applications, but the mapping does not have an explicit inverse, which is a slight practical complication [30].

The Legendre polynomials, widely used in high-order finite elements and "spectral elements", and also the Chebyshev polynomials are but special cases of the larger family of "Gegenbauer" or "ultraspherical" polynomials which are defined as the polynomials orthogonal on $x \in [-1, 1]$ with the weight function $(1 - x^2)^m$. The Chebyshev polynomials are the special case $m = -1/2$ while the Legendre polynomials are $m = 0$. The ultraspherical polynomials of integer m are factors in the associated Legendre functions, which are the latitudinal parts of the two-dimensional basis functions known as spherical harmonics. These are a good basis set for the latitude-and-longitude dependence in spherical coordinates and are widely used in weather forecasting and climate modeling.

The Hermite functions have asymptotic approximations for large degree n in terms of sine and cosine functions as discussed in Sect. 12.2 below.

Each species of basis function is associated with a canonical interval such that the least-squares spectral approximation is tailored to that interval. This will be dubbed the "expansion interval" in what follows.

In view of these connections, it is not surprising that there are great similarities between the asymptotic coefficient theories for many different species of orthogonal functions. However, there are some interesting differences, too, that we will illuminate below.

3 Integration-by-parts

By repeatedly integrating-by-parts—always *integrating* $\phi_n(x)$ and *differentiating* $f(x)$—one can derive an asymptotic series in inverse powers of n for Fourier series, rational Chebyshev functions, Legendre polynomials, Hermite functions, spherical harmonics and so on. There are, however, some subtleties.

The first is that the inverse power series in n are usually *asymptotic* but *divergent* (though it is easy to find special cases which converge). The reason is that a factor like $\exp(-\mu n)$, which appears in most spectral coefficient asymptotics, is not analytic in $1/n$, and so can never be approximated by a series of negative powers of n. (Put another way, in terms of $\nu \equiv 1/n$, $\exp(-\mu/\nu) \sim 0 + 0\nu + 0\nu^2 + \cdots$ because all derivatives of the function are zero at $\nu = 0$ so that the exponential has only the trivial (and useless) power series about the origin in ν.)

The second complication is that it may be possible to integrate-by-parts only a finite number of times because $f(x)$ is singular on the interval, and an integral with a sufficiently high derivative of $f(x)$ is non-integrable. The spectral coefficients always have a finite algebraic index of convergence in this case. If a periodic function has a square root branch point proportional to $\sqrt{x - x_0}$, for example, then the second derivative of $f(x)$ has a non-integrable singularity proportional to $1/(x - x_0)^{3/2}$. It follows that for such functions, it is only possible to integrate by parts a single time because a second integration by parts would generate an unbounded integral.

When only a finite number of integrations-by-parts are possible, it is still possible to extract a useful bound on the Fourier coefficients as follows.

Theorem 1 (Integration-by-parts coefficient bound) *If*

1.

$$f(\pi) = f(-\pi),\ f^{(1)}(\pi) = f^{(1)}(-\pi), \ldots, f^{(k-2)}(\pi) = f^{(k-2)}(-\pi), \tag{16}$$

2. $f^{(k)}(x)$ *is integrable,*

then the coefficients of the Fourier series

$$f(x) = a_0 + \sum_{n=1}^{\infty} a_n \cos(nx) + \sum_{n=1}^{\infty} b_n \sin(nx) \tag{17}$$

have the upper bounds

$$|a_n| \leq F/n^k; \qquad |b_n| \leq F/n^k \tag{18}$$

for some sufficiently large constant F, which is independent of n.

An equivalent way of stating the theorem is that, if the two conditions above are satisfied, then the algebraic index of convergence is at least as large as k.

Notes: (a) $f^{(k)}$ *denotes the k-th derivative of f(x). (b) The integrability of* $f^{(k)}$ *requires that* $f(x)$, $f^{(1)}(x), \ldots,$ $f^{(k-2)}(x)$ *must be continuous.* (From [1, Chap. 2], which also furnishes a proof.)

The third complication is that the leading-order asymptotic approximation to a_n sometimes involves *fractional* inverse powers of n. For $f(x)$ with a square-root singularity, the coefficient bound implies correctly that a_n and b_n are bounded by a constant divided by n. In actuality, though, the coefficients are decreasing proportional to $n^{-3/2}$ so that the bound is true but imprecise. In later sections, we shall describe a more precise tool for calculating the asymptotic Fourier coefficients of such a function.

The fourth complication is that for some basis sets such as Hermite functions, the integration-by-parts series *generically* includes *fractional* powers, regardless of the type of singularity. The n-th normalized Hermite function, $\psi_n(x)$, is the product of $\exp(-[1/2]x^2)$ with the normalized Hermite polynomial of degree n, $\overline{H}_n(x)$. The identity

$$\int^x \overline{H}_n(y)\mathrm{d}y = \frac{\overline{H}_{n+1}(x)}{\sqrt{2n+2}} \tag{19}$$

implies that each time we integrate-by-parts, integrating just the Hermite polynomial and differentiating the rest of the integral, we obtain only a factor proportional to the *square root* of n instead of n itself. One integration-by-parts gives explicitly

$$a_n = \left.\frac{f(x)\exp(-[1/2]x^2)\overline{H}_{n+1}(x)}{\sqrt{2n+2}}\right|_{-\infty}^{\infty} - \frac{1}{\sqrt{2n+2}}\int_{-\infty}^{\infty}\left[\frac{\mathrm{d}f}{\mathrm{d}x} - xf(x)\right]\overline{H}_{n+1}(x)\exp(-[1/2]x^2)\mathrm{d}x. \tag{20}$$

Just as for a Fourier series, further integrations-by-parts are only legitimate if $f(x)$ has sufficient differentiability, but there is also the additional constraint that the infinite integral is bounded. One can prove [31] the following.

Theorem 2 *If* $f(x)$ *is such that* $\mathrm{d}^j f/\mathrm{d}x^j$ *and* $x^j f(x)$ *(and all derivatives and moments of smaller* j*) are bounded and integrable on* $[-\infty, \infty]$*, then the normalized Hermite coefficients* a_n *of* $f(x)$ *satisfy*

$$|a_n| \leq C/n^{j/2}, \tag{21}$$

for some constant $C > 0$ *and all* $n > 0$ [31]. *If* $f(x)$ *decays exponentially fast as* $|x| \to \infty$ *and is infinitely differentiable for all real x, then the bound applies for arbitrarily large* j *and the convergence of the Hermite coefficients is "beyond-all-orders".*

This is very similar to its Fourier counterpart except that (i) each additional derivative increases the bound by $\sqrt{n}$ instead of a factor of n and (ii) all boundary terms vanish only if $f(x)$ decays exponentially fast, an extra constraint similar to the Fourier requirement that $f(x)$ be periodic.

In later sections, we shall develop tools more precise than integration-by-parts for asymptotically approximating spectral coefficients. First, though, we must develop some essential preliminary ideas.

4 Darboux's Principle and singularity matching

Theorem 3 (Darboux's Principle: singularities and convergence) *For all types of spectral expansions* (*and for ordinary power series*), *both the* DOMAIN *of* CONVERGENCE *in the complex plane and also the* RATE *of* CONVERGENCE *are controlled by the* LOCATION *and* STRENGTH *of the* GRAVEST SINGULARITY *in the complex plane. "Singularity" in this context denotes poles, fractional powers, logarithms and other branch points, and discontinuities of* $f(c)$ *or any of its derivatives.*

Each such singularity gives its own additive contribution to the coefficients a_n *in the asymptotic limit* $n \to \infty$. *The "gravest" singularity is the one whose contribution is larger than the others in this limit; there may be two or more of equal strength.*

For the special case of power series, this is "Darboux's Theorem" [8,32–35]. *It is discussed for other types of series in* [1, Chap. 2] *and* [36,37] *and Laguerre functions in* [38].

There are some apparent exceptions: *the rate of convergence of a Fourier series may be controlled by a failure of periodicity, and the rate of Hermite function convergence may be dominated by the rate at which* $f(x)$ *decays on the real axis. However, these exceptions are in fact always associated with singularities*: *the Fourier series of a non-periodic function converges to a function which is singular at the endpoints, and the rate of decay as* $x \to \infty$ *is associated with the singularity at infinity.*

Darboux's Principle can be reversed; there is now a cottage industry that uses the asymptotic behavior of numerically computed spectral coefficients to track the behavior of singularities in the complex-plane, especially with the goal of understanding how such singularities move onto the real axis [39–44].

When a spectral method is applied with a change of mapping $x(y)$, the mapping can be manipulated to move the convergence-limiting singularities farther from the expansion interval and thereby accelerate the rate of convergence as illustrated in [45–48]. Conversely, a change-of-coordinate that moves complex-plane singularities closer to the expansion interval in the new coordinate will deaccelerate convergence as illustrated on [1, pp. 334–338].

Darboux's Principle justifies the assertion made in Sect. 2: the smoother $f(x)$, the faster the convergence of its spectral series. Table 1 catalogues the relationship between the type of a singularity (logarithm, square root, etc.) and the asymptotic spectral coefficients.

Darboux's Principle implies a corollary that clarifies the Method of Model Functions.

Corollary 1 (singularity-matching) *If two functions* $f(z)$ *and* $g(z)$ *have convergence-limiting singularities of the same type and strength, then their asymptotic spectral coefficients are the same in the limit* $n \to \infty$. *If* $f(z) - g(z)$ *is singular, but more weakly singular than either* $f(z)$ *or* $g(z)$, *the difference between the spectral coefficients of* $f(z)$ *and* $g(z)$ *decreases as an algebraic function of the degree* n. *If* $f(z) - g(z)$ *is not singular at the location of the common gravest singularity of* $f(z)$ *and* $g(z)$, *then the difference between the spectral coefficients of* $f(z)$ *and* $g(z)$ *decreases exponentially fast with* n.

This corollary is a direct consequence of Theorem 3: If we can compute asymptotic expansions for the series coefficients which depend only on the gravest singularity, then when the singularity is eliminated by taking the difference $f(z) - g(z)$, the leading term in the asymptotic approximation for the spectral coefficients is also eliminated. The spectral series for the difference must therefore converge more rapidly than the expansions for the more singular functions $f(z)$ and $g(z)$.

This corollary defines in what sense an explicit model function should resemble the unknown solution to a differential equation: The model and the unknown $u(x)$ should have the same gravest, convergence-limiting singularities.

Illustrations of Darboux's Principle are given in [1, Chap. 2] and also in [49]. A new example is furnished here by comparing three functions which are quite different in shape (left panel of Fig. 1):

$$f_1 = \frac{2a}{x^2 + a^2}, \tag{22}$$

$$f_2 = 5\sin(10x)\exp(x/2) + \frac{2a}{x^2 + a^2}, \tag{23}$$

Table 1 Relationships between singularities and asymptotic spectral coefficients

Form of singularity	Type of singularity	Asymptotic form spectral coefficients
$1/(x-a)$	Simple pole	$[\,]p^n$
$1/(x-a)^2$	Double pole	$[\,]n\ p^n$
$\log(x-a)$	Logarithm	$[\,]n^{-1}\ p^n$
$1/\sqrt{x-a}$	Reciprocal of square root	$[\,]n^{-1/2}\ p^n$
$(x-a)^{1/3}$	Cube root	$[\,]p^n/n^{4/3}$
$\exp(-q/\lvert x\rvert)$	Infinitely differentiable but singular at $x=0$	$[\,]\ \exp(-pn^{1/2})$
$f(x)=\text{sign}(x)$	Jump discontinuity	$[\,]\ /n$
$\mathrm{d}f/\mathrm{d}x=\text{sign}(x)$	Discontinuous first derivative (assuming f continuous)	$[\,]\ /n^2$
$\lvert x-x_0\rvert^\psi$	Branch point within [−1,1]	$[\,]\ 1/n^{\psi+1}$
$\lvert x-x_0\rvert^\psi \log^p(\lvert x-x_0\rvert)$	Log point within [−1,1]	$[\,]\ \log^p(n)/n^{\psi+1}$
Endpoint singularities: Chebyshev only		
$(1-x)^\psi$	Branch point at endpoint	$[\,]\ 1/n^{2\,\psi+1}$
$(1-x)^\psi \log(1-x)$	Branch point at endpoint	$[\,]\ \log(n)/n^{2\,\psi+1}$
$\exp(-q/\lvert x+1\rvert)$	Infinitely differentiable but singular at endpoint	$[\,]\ \exp(-p\,n^{2/3})$

Note. All rows, except the last three, apply to Fourier series as well as Chebyshev polynomials. The constant $p=\exp(-a)$. The empty brackets in column three denote an unspecified constant

$$f_3=\frac{10(1+x)\cos(5x)}{x^2+2a^2}+\text{sech}\left(\frac{\pi}{2a}x\right). \tag{24}$$

The lower-degree ($n<20$) Chebyshev coefficients of these three functions also differ greatly (right panel of Fig. 1). However, because the nearest-the-real-axis singularities of these functions are in the same location, all simple poles, and with the same residue, the Chebyshev coefficients for all three are *asymptotically equal* as $n\to\infty$.

This theorem implies that the examples below are not merely special cases. Rather, each is typical of a whole *class* of functions that have singularities of the same type at the same point. For example, denoting an arbitrary complex parameter by a, $1/(x+a)$ is representative of all functions whose convergence is limited by a first order pole at $x=-a$.

One minor subtletly is that for a multiply branched function, each branch has its own expansion/s whose convergence is controlled only by singularities on that branch. For example, the Lambert W-function, which is defined implicitly as the solution of $W\exp(W)-x=0$, has two real-valued branches [50]. On the principal branch, denoted $W_0(x)$ and defined for $x\in[-\exp(-1),\infty]$, one can expand $W_0(x)$ as a power series about $x=0$ which converges for $\lvert x\rvert<1/\exp(1)$, and likewise make exponentially convergent Chebyshev expansions on any interval that does not include the endpoints $x=-\exp(-1),\infty$ where $W_0(x)$ is singular. It is not possible to expand the other real-valued branch, $W_{-1}(x)$, defined only for $x\in[-\exp(-1),0]$ in a power series about $x=0$ because this branch is singular (in fact, infinite) at that point. Each branch must be treated as if a different, independent function: the singularities and properties of spectral series may be different on different Riemann sheets.

5 Poisson summation, imbricate series, and all that

It is hardly a secret that there is a close relationship between Fourier series and Fourier Transforms. A more precise expression of this connection, rarely taught in undergraduate math classes, is the following.

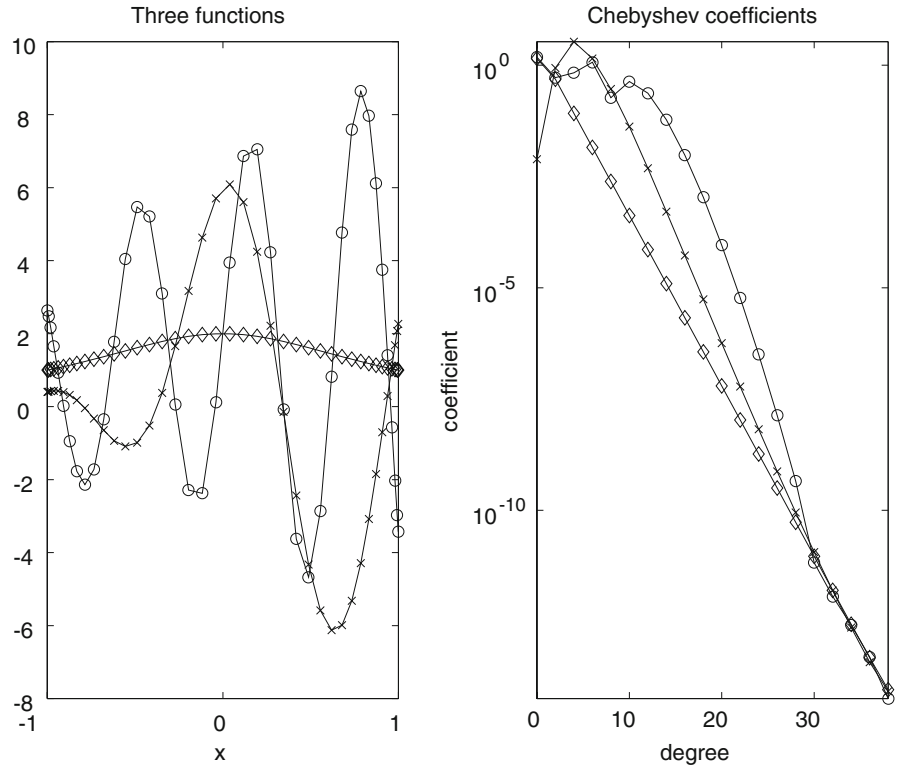

Fig. 1 Left: the functions f_1 (diamonds), f_2 (circles) and f_3 (x's) for $a = 1$ where each function is defined in the text. Right: the Chebyshev coefficients for these three functions. Although each function is very different in appearance (*left*), they all have convergence-limiting singularities of the same location and residue, so their spectral coefficients are ASYMPTOTICALLY the same as $n \to \infty$ (*right*)

Theorem 4 (Poisson summation/imbricate series) *Any periodic function with period L has the two series representations*

$$f(x) = \sum_{n=-\infty}^{\infty} g(n)\ \exp(\mathrm{i}nx) = \sum_{m=-\infty}^{\infty} G\left([x - 2\pi m]\right), \tag{25}$$

where the series on the left is the usual (*complex*) *Fourier series, the series on the right is the "imbricate" series, and where* $G(k)$ *and* $g(x)$ *are Fourier transforms of one another*:

$$G(k) = \int_{-\infty}^{\infty} g(x) \exp(\mathrm{i}kx)\ \mathrm{d}x, \tag{26}$$

$$g(x) = \frac{1}{2\pi} \int_{-\infty}^{\infty} G(k) \exp(-\mathrm{i}kx)\ \mathrm{d}k. \tag{27}$$

The theorem is valid if (i) $G(k) \in \mathcal{L}^1(R)$, *that is, if the integral of the absolute value of* $G(k)$ *over the entire real axis is bounded and also* (ii) $g(x) = O\left((1 + |x|)^{-\alpha}\right)$ *as* $|x| \to \infty$ *for some* $\alpha > 1$.

In words, the Poisson summation theorem implies that every Fourier series has an alternative representation as the periodization or "imbrication" of a "pattern function" $G(x)$. The pattern function is the Fourier transform of $g(n)$, the coefficients of the Fourier series.

To understand the effect of a certain type of singularity on the Fourier coefficients, we can choose a pattern function with the required singularity, and then the Fourier transform of $G(x)$ yields the corresponding Fourier coefficients. (Note that it is often easier to evaluate the infinite integral which defines the Fourier transform than the

finite integral, with endpoint effects, that defines the Fourier coefficients.) Alternatively, one can solve the inverse problem of determining singularity type from the Fourier coefficients by taking the transform of the coefficient function $g(x)$.

For example, an obvious inverse question is: if the Fourier coefficients are asymptotically proportional to n^{-2m} for some m, what is the corresponding singularity in $f(x)$? Now the function n^{-2m} is singular at the origin, and unsuitable, but all that is really needed is a function $g(n)$ which *asymptotes* to a power law. We therefore choose

$$g(n) = \frac{1}{(n^2 + a^2)^m} \to G(x) = \frac{\sqrt{\pi}}{\Gamma(m)2^{m-3/2}} \frac{x^{m-1/2}}{a^{m-1/2}} K_{m-1/2}(xa), \tag{28}$$

where K_ν is the usual Bessel function. From the known properties of $K_{m-1/2}$, there is a discontinuity of the derivative of order $(2m-1)$ when m is an integer; thus n^{-2} decay of the coefficients implies a discontinuous first derivative, n^{-4} decay a discontinuous third derivative and so on. There is a branch point proportional to $|x|^{2m-1}\log(|x|)$ when m is a half-integer; thus, n^{-3} implies a singularity of the form $x^2\log(|x|)$, Lastly, there is a branch point proportional to $|x|^{2m-1}$ when m is neither an integer nor a half-integer.

Sir James Lighthill's book on Fourier series and transforms contains a short table connecting singularities to asymptotic behavior of spectral coefficients, derived through similar reasoning. We shall give an expanded version of his table below.

6 Singularity location and the unimportance of phase shifts

In real estate, the mantra is "Location! Location! Location!": A three-bedroom condominium costs at least five times as much in Manhattan or Honolulu as in rural Iowa. The same principle applies for spectral series, too: the rate of convergence of the series for $f(x)$ is completely controlled by the location and type of singularities—poles, branch points, discontinuities, etc.—of $f(x)$ in the complex x-plane. The location is far more important than singularity type because location completely determines the asymptotic rate of geometric convergence. To quantify this, we need some tools.

Definition 1 (*Asymptotic rate of geometric convergence*) If

$$\log(|a_n|) \sim -\mu n + \text{lower order} \tag{29}$$

then μ is the "asymptotic rate of geometric convergence".

Theorem 5 (Singularity location and rate of convergence) *If a function $f(x)$ has a singularity at a point x_s, then for Fourier, Chebyshev, Legendre and Gegenbauer bases, this will contribute a term $s(n)\exp(-\mu(x_s)n)$ to the asymptotic spectral coefficients of f where μ depends, for a given spectral basis, only on x_s and not on the type of singularity or other properties of $f(x)$ and where $s(n)$ is a factor that varies more slowly with n than the exponential. The asymptotic rate of geometric covergence is the minimum of the $\mu(x_s)$ for each of the singularities of $f(x)$. The non-exponential factor $s(n)$ does depend on the type of singularity.*

A proof and expanded discussion is given in [1] and [51].

Definition 2 (*Isoconvergence contours*) For a given spectral basis, the curves of constant $\mu(x)$ in the complex x-plane are "isoconvergence" contours in the sense that a singularity anywhere on an isoline of μ will contribute the same asymptotic rate of geometric convergence to the spectral series of $f(x)$.

Theorem 6 *For a Fourier series, the isoconvergence contours are lines parallel to the real axis; the asymptotic rate of convergence $\mu(x)$ contributed by a singularity of $f(x)$ at x is*

$$\mu(x) = |\Im\mathfrak{m}(x)| \quad \text{[Fourier]}. \tag{30}$$

For Chebyshev, Legendre and Gegenbauer polynomials, the isoconvergence contours are ellipses in the complex x-plane with foci at $x = \pm 1$ with

$$\mu = \Im\mathrm{m}(\arccos(x)) \tag{31}$$

$$= \log|x \pm \sqrt{x^2-1}| \tag{32}$$

$$= \log\left(\alpha + \sqrt{\alpha^2-1}\right) \tag{33}$$

where the sign in the second line is chosen to make the argument of the logarithm larger than one and where

$$\alpha \equiv \frac{1}{2}\sqrt{(\Re\mathrm{e}(x)+1)^2 + (\Im\mathrm{m}(x))^2} + \frac{1}{2}\sqrt{(\Re\mathrm{e}(x)-1)^2 + (\Im\mathrm{m}(x))^2}. \tag{34}$$

Proof [1, Chap. 2] and also [51].

Instead of recapitulating the formal proofs, it is more illuminating to proceed heuristically. A spectral series must fail at a singularity because if $f(x)$ or any of its derivatives is infinite, then the series can approximate $f(x)$ at and near the singularity only by diverging. The basis functions $\{\cos(nx), \sin(nx)\}$ of a Fourier series grow as $\exp(n|\Im\mathrm{m}(x)|)$ away from the real axis. If the coefficients are bounded by a constant times $\exp(-n\mu)$, then the series will converge geometrically in the strip $|\Im\mathrm{m}(x)| < \mu$ and diverge geometrically for larger $|\Im\mathrm{m}(x)|$. But how is μ related to the distance to the singularity? The answer is: as favorably as possible: A Fourier series converges in the largest strip, centered on the real x-axis, which is singularity free.

In the previous section, the example of a function with singularities at $x = 0$ would seem to be rather special because singularities may in general be located at any x. However, there is no real loss of generality in specializing to singularities located at the origin: shifting the location of the convergence-limiting singularity parallel to the real axis causes *oscillations* in degree n, but has *no effect* on their *decay* as expressed by the following.

Theorem 7 (Fourier translational shift) *Define*

$$g(x) \equiv f(x+s) \tag{35}$$

and suppose

$$f(x) = \sum_{j=0}^{\infty} A_j \cos(jx) + \sum_{j=1}^{\infty} B_j \sin(jx). \tag{36}$$

Then the coefficients in the series

$$g(x) = \sum_{j=0}^{\infty} a_j \cos(jx) + \sum_{j=1}^{\infty} a_j \sin(jx) \tag{37}$$

are

$$a_j = \cos(js)A_j + \sin(js)B_j, \tag{38}$$

$$b_j = \cos(js)B_j - \sin(js)A_j. \tag{39}$$

The elliptical equiconvergence contours for Chebyshev polynomials are consequences of the mapping $x = \cos(t)$ that connects a Fourier cosine series to a Chebyshev series through $T_n(\cos(t)) = \cos(nt)$: each pair of lines $\Im\mathrm{m}(t) = \pm\mu$ is mapped into an ellipse in the complex x-plane where μ does double-duty as the elliptical coordinate in the transformation $\Re\mathrm{e}(x) = \cosh(n\mu)\cos(n\eta)$, $\Im\mathrm{m}(x) = \sinh(n\mu)\sin(n\eta)$. The polar angle η is as irrelevant for Chebyshev series as $\Re\mathrm{e}(x)$ is for Fourier series: the rate of convergence depends only on μ, that is, only on the distance from the interval $x \in [-1, 1]$ of the ellipse which contains the singularity.

The Legendre and Gegenbauer polynomials, closely related to the Chebyshev polynomials, all have the same asymptotic rate of geometric convergence for a given $f(x)$. However, when the polynomials are normalized, the factor $s(n)$ is larger for the Gegenbauer polynomials of superscript m than for Chebyshev by a factor of $n^{m-1/2}$, and the Legendre slowly-varying factor is larger than its Chebyshev counterpart by a factor of $\sqrt{n}$ [52,53].

7 Asymptotics-by-example

Once Darboux's Principle and the importance of singularity is understood, one can fill in much of Table 1 by using mathematical handbooks to identify examples with known expansions. All functions whose convergence-limiting singularity is a simple pole at a particular location will have the same asymptotic spectral coefficients as the *simplest* function with such a pole and such a residue at such a location.

Thus, the asymptotic effect of poles and power-law branch points on Fourier series can be understood from, defining $q = \pi^{-3/2} a^{1-2m} \cos(\pi m)\Gamma(1-m)$,

$$\Lambda(x;\, p) \equiv \sum_{m=-\infty}^{\infty} 1 \,/\, [\,(x - 2\pi m)^2 + a^2]^m \tag{40}$$

$$= q\{\Gamma(m - 1/2)/2 + 2^{3/2-m} \sum_{n=1}^{\infty} n^{m-1/2} K_{m-1/2}(an) \cos(nx)\} \tag{41}$$

where $K_\nu(z)$ is the imaginary Bessel function. Since

$$n^{m-1/2} K_{m-1/2}(an) \sim (\pi/[2a])^{1/2} n^{m-1} \exp(-an)\{1 + m(m-1)/(2an) + \cdots\} \tag{42}$$

for $n \gg m^2$, it follows that fractional powers (non-integral m) follow the same rules as poles (m a positive integer).

If the parameter a is real, the singularities of this exemplar are on the imaginary axis at $x = \pm ia$, but as explained earlier, there is no loss of generality because shifting the singularities parallel to the real axis merely induces oscillations in n as expressed by Theorem 7. By substituting $z = \arccos(x)$, the example turns into a Chebyshev series.

The books of Yudell Luke [54,55], Geza Németh [56] and Martin Snyder [57] etc., are full of examples which can be used in a similar way to connect many species of singularities to the asymptotic Chebyshev and Fourier coefficients. Indeed, this strategy is so effective that much work on the spectral effects of poles and branch points has been "look-up" asymptotics rather than "asymptotics-by-derivation".

However, asymptotic methods for integrals, applied to the usual integrals for spectral coefficients, are quite essential for functions that are C^∞ on the expansion interval—singular, but in such a way that the function is infinitely differentiable with bounded derivatives even at the point of singularity. Furthermore, asymptotic methods like steepest descent have historically been used to bypass the use of Darboux's Principle and the Method of Model Functions to compute the consequences of a pole or branch point directly, especially in the work of David Elliott and his collaborators [58–63], Jet Wimp [64,65], and Géza Németh [56].

8 Steepest descent for integrals

Suppose we need to asymptotically approximate the integral

$$I(n) \equiv \int_a^b \exp(\Phi(z, n)) s(z) \mathrm{d}z \tag{43}$$

as $n \to \infty$. Suppose that the integrand has a so-called "stationary point" z_s where

$$\frac{\mathrm{d}\Phi}{\mathrm{d}z}(z_s) = 0, \tag{44}$$

such that, as n increases, the integrand becames more and more sharply peaked about the stationary point. ("Sharply peaked" implicitly requires that the curvature at the stationary point is negative if $\exp(\Phi(z_s, n)$ is positive.) The increasing narrowness of the peak of the integrand makes it possible to approximate the integral by means of a local Taylor expansion around the stationary point. In order to capture the finite width of the peak, it is necessary to expand the "phase function" Φ to at least second order; the first-order term is zero because z_s is a stationary

point. The non-exponential factor $s(z)$ varies less and less over the width of the peak in $\exp(\Phi(z,n))$ and thus can be approximated by its value at the stationary point, giving

$$I(n) \approx \exp(\Phi(z_s,n)s(z_s) \int_a^b \exp(\Phi_{zz}(z_s,n)(z-z_s)^2/2)\mathrm{d}z, \tag{45}$$

where Φ_{zz} is the second derivative of Φ; the negative curvature assumption requires that $\Phi_{zz}(z_s) < 0$. Because the integrand is sharply peaked about the stationary point and the approximate Gaussian integrand is exponentially small at the integration limits (a, b), only an exponentially small error is made by extending the limits of integration to infinity. Then, analytically evaluating the integral of a Gaussian on an infinite interval,

$$I(n) \approx \sqrt{2\pi}\ \exp\{\Phi(z_s,n)\}\ s(z_s)\ \frac{1}{\sqrt{-\Phi_{zz}(z_s)}}. \tag{46}$$

If there are multiple stationary points on the steepest-descent path, the approximation is a sum over the contributions of each point.

The good news is that the Fourier transform integral, which we can use through the Poisson Summation Theorem to deduce properties of Fourier series, is an infinite integral with an exponential function $\exp(inz)$ that does indeed vary faster and faster as $n \to \infty$. The bad news is that the exponential has an imaginary argument, and therefore is not of quite the right form.

Fortunately, the path of integration can be deformed into the complex plane without altering the integral, as long as the contour is not moved across a singularity of the integrand. Indeed, the contour can be moved across singularities as long as the contributions of these singularities are added to the integral along the new path. The algorithm is called "steepest descent" because the deformed integration contour is chosen so that the integrand falls as fast as possible from its maximum at the stationary point.

Ironically, the steepest-descent path does not explicitly appear in the approximation to the integral. A transcendental function $\Phi(z)$ may have an infinite number of roots of its first derivative; the steepest-descent path is important only to show that a steepest-descent contour that passes through the endpoints of the original integration path can be found, and also to identify which stationary points actually lie on the integration path.

A full discussion with many examples is given in texts such as [66,67] and the review [6]. But it is best to illustrate with a concrete example as furnished in the next section.

9 C^∞ singularities

9.1 Definition

Weak singularities such that a function is infinitely differentiable with bounded derivatives at a point x_{sing} and yet is not analytic there in the sense of complex variable theory—C^∞ but not C^Ω is mathematical jargon—are surprisingly common in applications. First, functions on a semi-infinite or infinite interval *generically* have such singularities at infinity. Second, C^∞ functions on a finite interval are very useful for applying a Fourier series to a nonperiodic problem [68], embedding an irregular domain within a periodic rectangle [69], creating infinitely differentiable windows [70] and so on. Third, many special functions $f(z)$ like Bessel functions are computed for large z by using asymptotic inverse powers of z. With the change of coordinate $x = 1/z$, these become asymptotic power series in x for a function that is C^∞ but singular at $x = 0$. In this section, we will confine attention to C^∞ singularities at a finite x and discuss the special challenges of unbounded intervals in the next section.

9.2 Functions with trivial power series about the singular point

The function

$$f(x) \equiv \exp(-A/x), \tag{47}$$

where A is a constant with $\mathfrak{Re}(A) > 0$ has only the trivial power series,

$$\exp(-A/x) \sim 0 + 0x + 0x^2 + \cdots \tag{48}$$

because all its derivatives are zero at the origin. However, this same $f(x)$ has a series of Chebyshev polynomials that converges exponentially fast to the function.

The coefficients in the series

$$\exp(-A/x) = \sum_{n=0}^{\infty} a_n T_n(2x-1), \quad x \in [0,1] \tag{49}$$

are given by

$$a_n = \frac{2}{\pi}\int_0^1 \exp(-A/x)\, T_n(2x-1)\frac{1}{\sqrt{x(1-x)}}\mathrm{d}x, \quad n \geq 1. \tag{50}$$

Because Fourier coefficient integrals are easier to work with than Chebyshev coefficient integrals, the first step is to write the coefficient integral without approximation as

$$a_n = \frac{2}{\pi}\,\mathfrak{Re}\left\{\int_0^{\pi} \exp(-2A/(1+\cos(t)) + \mathrm{i}nt)\mathrm{d}t\right\}. \tag{51}$$

Define the steepest-descent phase function

$$\Phi = -2A/(1+\cos(t)) + \mathrm{i}nt. \tag{52}$$

The stationary points t_s are then the roots of the transcendental function

$$\frac{\mathrm{d}\Phi}{\mathrm{d}t} = \mathrm{i}n - \frac{2A\sin(t)}{(1+\cos(t))^2}. \tag{53}$$

This equation has no simple analytic solutions but, fortunately, it is usually possible to make approximations as $n \to \infty$. In particular, when $n \gg 1$, the trigonometric term can cancel in in (54) only when the denominator of the trigonometric term is very close to zero. This justifies a Taylor expansion about $t = \pi$ (which is the image of the singular point $x = 0$):

$$\frac{\mathrm{d}\Phi}{\mathrm{d}t} \approx \mathrm{i}n + \frac{8A}{(t-\pi)^3}. \tag{54}$$

This cubic has three roots. To choose the correct root, we have to think about the steepest-descent path.

First, observe that $\exp(\mathrm{i}nt)$ decays as $\mathfrak{Re}(t)$ increases in the upper half-plane, so the steepest-descent path will likely lie in the upper half-plane. The integrand is zero at $t = \pi$; a steepest-ascent path will be parallel to the real axis, moving towards smaller t, and then bend upward as it begins to feel the influence of the $\exp(\mathrm{i}nt)$. The path will eventually run parallel to the imaginary axis to $\mathrm{i}\infty$ where a segment at infinity connects to a return down the imaginary axis. It follows that the only stationary point on the path of integration is that for which (i) $\mathfrak{Im}(t_s) > 0$ and $\mathfrak{Re}(t_s) < \pi$:

$$t_s \approx \pi + 2A^{1/3}\frac{1}{n^{1/3}}\exp(\mathrm{i}\pi(5/6)). \tag{55}$$

One can confirm this choice by plugging each of the three stationary points into $\Phi(t)$: since the Chebyshev coefficients decay exponentially with n, all stationary points that give a $\Phi(t_s)$ that *grows* with n can be rejected.

Substituting in (47), making Taylor expansions about t_s, and a little algebra, yields

$$\begin{aligned} a_n \sim\ & 4(-1)^n\sqrt{\frac{1}{3\pi}}A^{1/6}n^{-2/3}\exp\left\{-(3/2)A^{1/3}n^{2/3} - A/3\right\} \\ & \times \cos\left\{\sqrt{3}(3/2)A^{1/3}n^{2/3} - \pi(5/3)\right\}, \qquad n \gg 1. \end{aligned} \tag{56}$$

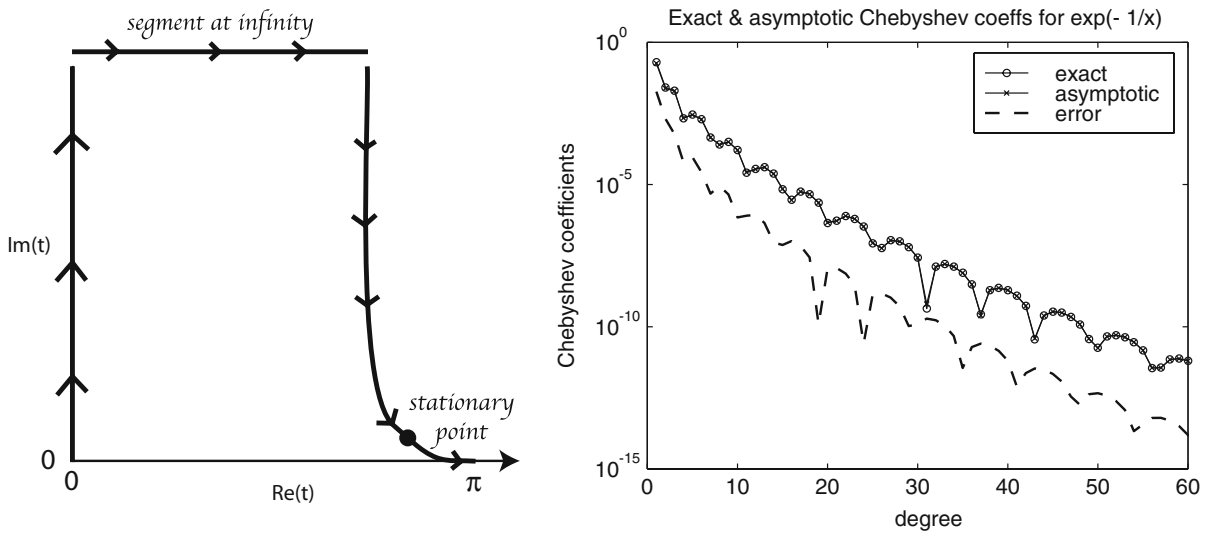

Fig. 2 *Left*: schematic of the steepest-descent path for asymptotically approximating the Chebyshev coefficients of $\exp(-A/x)$ on the interval $x \in [0, 1]$. Note that the Chebyshev coefficient integral is first converted to the equivalent cosine integral in t through the change of coordinate $x = \cos(t)$. The black disk is the stationary point; short arrows show the direction of integration. The horizontal segment is actually located at infinity in the upper half-plane, but is depicted as a horizontal line at a finite vertical distance; the path of integration is broken below the segment to indicate the ungraphable vertical segments of infinite extent. *Right panel*: exact Chebyshev coefficients for $f(x) = \exp(-1/x)$ (circles), the asymptotic coefficients (x's) and the error which is the difference between these curves (dashed)

Figure 2 shows the steepest-descent path (left) and the comparison between the exact and asymptotic Chebyshev coefficients on the right. The steepest-descent approximation can be extended to a full asymptotic series as described in [6,66,67].

There are a couple of subtleties. First, the contribution from the stationary point t_s is only an approximation to the integral on *part* of the path, namely, on the segment from infinity to $t = \pi$ through the stationary point. The integral from $t = 0$ to $t = \mathrm{i}\infty$ is not in any sense approximated by the steepest-descent formula because the integrand has *two* maxima on the path of integration, one at t_s and the other at $t = 0$. However, it is easy to show that because the integrand is purely real on the imaginary axis, the complex path integral on the imaginary axis is *pure imaginary* and therefore disappears when we take the real part.

Second, standard texts usually write the phase function as a linear function of the large parameter, and relegate everything not multiplied by n to the slowly-varying function $s(z)$. Unconventionally, we have defined the "phase function" as $\exp(\Phi(t)) \equiv \exp(-2A/(1+\cos(t)) + \mathrm{i}nt)$. It is not possible to obtain sensible results from treating $\exp(\mathrm{i}nt)$ as the only rapidly varying part of the integrand because $\exp(-2A/(1+\cos(t)) \approx \exp(-A/3)\exp(-4A/(t-\pi)^2)$ for t near π. which implies that this exponential factor is always varying more rapidly than $\exp(\mathrm{i}nt)$—not slower—sufficiently close to $t = \pi$. The stationary point t_s is jointly controlled by both factors in the exponential; t_s is proportional to $n^{-1/3}$, which magnifies the importance of $\exp(-2A/(1+\cos(t))$ as n increases even though $\exp(\mathrm{i}nt)$ is increasing with n also. This situation of an n-dependent stationary point, controlled in part by terms that do not *explicitly* depend on n, arises again and again in applying steepest descent to spectral coefficient integrals.

9.3 Functions with non-trivial power series

If a function is singular but infinitely differentiable at a point $x = 0$, it cannot have a *convergent* power series, but an *asymptotic* power series is perfectly possible. One useful class of examples are the "Stieltjes functions", important in applications as explained in [67]. These are defined to be all functions with an integral representation of the form

$$f(x) = \int_0^\infty \frac{\rho(t)}{1+xt}\,\mathrm{d}t, \tag{57}$$

where the function $\rho(t)$ is non-negative for $t \in [0, \infty]$ and all the moment integrals $b_n = \int_0^\infty t^n\,\rho(t)\mathrm{d}t$ exist.

The prototypical Stieltjes function is *the* Stieltjes function

$$S(x) = \int_0^\infty \frac{\exp(-t)}{1+xt}\,\mathrm{d}t = E_1(1/x)\exp(1/x)/x \sim \sum_{n=0}^{\infty}(-1)^n\,n!x^n. \tag{58}$$

George F. Miller, Jr., showed more than 40 years ago [71] that the coefficients a_n in the series

$$S(x/A) = \sum_{n=0}^{\infty} a_n T_n(2x-1) \tag{59}$$

are asymptotically

$$a_n \sim 4(-1)^n \sqrt{\frac{\pi}{3}} A^{1/2}\,\exp\left(-(3A^{1/3}n^{2/3} + A/3)\right). \tag{60}$$

Miller performed an exact transformation of the coefficient integral, and then applied steepest descent to obtain the asymptotic coefficients for a class of functions expressible in terms of confluent hypergeometric functions including the exponential integral and the error function. In passing, he notes that the expansion of $\exp(-A/x)$ can be deduced by taking the imaginary part of his (5.9); the result agrees with (56), derived here from the cosine coefficient integral instead.

9.4 Gevrey order and the exponential index of convergence

When a function is C^∞ but not analytic on the interval, the rate of convergence is "subgeometric" in the sense that the exponential index of convergence r is less than one where r is defined as follows.

Definition 3 The "exponential index of convergence" r is given by

$$r \equiv \varlimsup_{n\to\infty} \frac{\log|\log(|a_n|)|}{\log(n)}, \tag{61}$$

where $\varlimsup$ is the usual supremum limit.

An equivalent definition is that if s and $q > 0$ are constants and

$$a_n \sim O(s\exp[-qn^r]), \qquad n \gg 1, \tag{62}$$

then the exponential index of convergence is the exponent r. [1, p. 26].

It seems logical that r is somehow a function of the smoothness of the singularity that creates subgeometric convergence, but how can one classify singularities that are non-analytic, and yet infinitely differentiable? One useful concept is the following.

Definition 4 (*Gevrey order*) Suppose a function is C^∞ but not analytic at $x = 0$. Let b_n denote the coefficients of the asymptotic but divergent power series. Then the Gevrey order G is the smallest γ for which there is a bound on the power series coefficients of the form

$$|b_n| \le C\,(n!)^\gamma, \quad \forall n, \tag{63}$$

where C is a constant. An equivalent definition is

$$\varlimsup_{n\to\infty} \frac{\log|b_n|}{n\log(n)} = G. \tag{64}$$

(Note that similar but not always identical definitions of Gevrey order appear in the literature; our definition is that of Sibuya [72].)

There is no general theory connecting r and G. However, Boyd proved the following bounds on the exponential convergence index r.

Theorem 8 *If $f(x)$ is a function with a power series of Gevrey order G at $x = 0$ and r is the exponential convergence index of the coefficients of its Chebyshev series, $f(x) = \sum_{n=0}^{\infty} a_n T_n(2x-1)$, then*

$$r \le \frac{2}{G+2}. \tag{65}$$

If $f(x)$ belongs to the more limited class of Stieltjes functions, then

$$\frac{2}{G+2} \ge r \ge 1 - G/2, \tag{66}$$

[73,74].

The Stieltjes function is of Gevrey order one and the steepest-descent method shows that $r = 2/3$, the upper limit of the inequality. It is an open problem whether there are in fact examples where $r < 2/(G+2)$.

9.5 Subfactorial functions: zero Gevrey order

Boyd [75] analyzed a function that he called "subfactorial" in the sense that the power series for $f_{\rm sub}(x)$ has a zero radius of convergence, but the Gevrey order is zero. His example is

$$f_{\rm sub}(x) \equiv \int_0^{\infty} \frac{\exp(-\exp(t))}{1+xt}\,{\rm d}t \sim \sum_{n=0}^{\infty} b_n x^n = \sum_{n=0}^{\infty} a_n T_n(2x-1). \tag{67}$$

From steepest descent, the power-series coefficients b_n are asymptotically

$$\log(|b_n|) \sim n\left\{\log\left[\log(n) - \log(\log(n))\right] - \frac{1}{\log(n)}\right\} \tag{68}$$

which for very, very large n simplifies to $\log(|b_n|) \sim n\ \log(\log(n))$. For a power series of finite radius of convergence ρ, the logarithm of the power series asymptotes (in the sense of a supremum limit) to n/ρ, so the $\log(\log(n))$ factor implies that the power series of $f_{\rm sub}(x)$ has zero radius of convergence. However, the divergence is proportional to $\exp(n\log(\log(n)))$ instead of the $\exp(n\log(n))$ growth of coefficients for a series with $G = 1$, such as that for the Stieltjes function. Boyd shows that the Chebyshev coefficients asymptote to

$$|a_n| \sim 2\sqrt{2\pi}\, n^{-1/2} \log^{1/4}(n) \exp(\Phi), \tag{69}$$

where

$$\Phi \sim -n\left\{\frac{2}{\sqrt{\log(n)}} + \frac{\frac{3}{2}\log(\log(n)) + \frac{2}{3}}{\log^{3/2}(n)} + \frac{\frac{59}{60} - \frac{3}{4}\log(\log(n)) + \frac{27}{16}[\log(\log(n))]^2}{\log^{5/2}(n)}\right\}. \tag{70}$$

If $f(x)$ were free of singularities on the expansion interval so that the rate of convergence was geometric, then the expression in the curly braces for Φ would be, to lowest order, a constant. Instead, $a_n \sim s(n)\exp(-2n/\sqrt{\log(n)})$ to lowest order where $s(n)$ represents the slowly-varying non-exponential factors; these coefficients fail to converge geometrically only because of the $\sqrt{\log(n)}$ factor in the exponential. The concept of an "exponential index of convergence" is not useful because the Chebyshev series for the subfactorial function converges faster than any subgeometric series with $r < 1$, but at the same time is slower than any true geometric series ($r = 1$).

9.6 Superfactorial functions: $G = \infty$

Sir Michael V. Berry studied the power series of what he dubbed "superfactorial functions" [76] such as

$$f_{\text{sup}}(x; A) \equiv \sqrt{A/\pi} \int_0^\infty \frac{\exp(-A \log^2(t))}{1 + xt} \frac{\mathrm{d}t}{t}, \tag{71}$$

where $A > 0$ is a constant. Berry showed that by the substitution $t = \exp(u)$, the power-series coefficients are given *exactly* by

$$b_n = \exp(n^2/(4A)). \tag{72}$$

Thus, the power-series coefficients diverge proportional to *Gaussians* of n rather than any finite power of the factorial; the Gevrey order is therefore infinite.

Boyd [75] shows through steepest descent

$$a_n \sim \frac{2\nu z}{\sqrt{z + 2\mu + 1}} \exp\left(p_0 z^{-2} + p_1 z^{-1} + p_2 + \cdots\right), \tag{73}$$

where

$$\nu \equiv \frac{n}{4A}, \quad z \equiv \frac{1}{\log(\nu)}, \quad \mu \equiv \log(\log(\nu)), \tag{74}$$

$$p_0 = -4A, \quad p_1 = 2 - 8A + 8A\mu, \quad p_2 = 2\mu - 4A\mu^2. \tag{75}$$

The exponential index of convergence r is not useful for this extreme either because the superfactorial Chebyshev series converges more slowly than $\exp(-qn^r)$ for any $r > 0$. The leading term in the asymptotic series for a_n is $\exp(-4A \log^2(n))$, which decreases very slowly indeed!

10 Uniform and non-uniform asymptotics: optimizing a parameter

Before we proceed further to discuss infinite-interval problems, we must pause to consider an issue we have so far successfully avoided: many types of spectral expansions contain a parameter whose value is crucial to the practical success of the spectral expansion. For example, the Hermite functions $\psi_n(x)$ are a complete orthogonal basis set for the unbounded interval, $x \in [-\infty, \infty]$. However, for an arbitrary positive constant α, $\psi_n(\alpha x)$ is also a basis: when the infinite interval is stretched or compressed through the change of coordinate $x \to \alpha x$, the unbounded domain is unchanged and invariant. In a practical sense, the choice of the scaling parameter α is extremely important. If the goal is to approximation a function like $\exp(-1000x^2)\cos(100x)$, then $\alpha = 1$ will require an enormously large series because there is a huge mismatch between the $O(1)$ width of the lowest basis functions and the $O(1/100)$ length scale of $f(x)$.

One of the goals of spectral-coefficient asymptotics is to help us choose such parameters wisely. It turns out in almost all cases, however, that the best choice of α is *dependent on the truncation* N of the spectral basis: what is best for small N may be orders-of-magnitude different from what is optimum when N is huge.

For any spectral approximation that depends upon a parameter and any particular function $f(x)$, the error in an expansion truncated after the N-th term,

$$E(N, \alpha) \equiv \max_x \left| f(x) - \sum_{n=0}^{N} a_n(\alpha)\, \phi_n(x; \alpha) \right|, \tag{76}$$

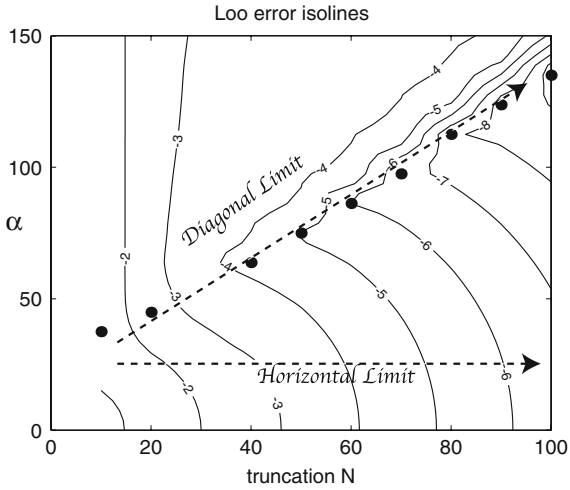

Fig. 3 Schematic of the contours of the logarithm of error for the expansion of a typical $f(x)$ in a basis that depends on a parameter α for various truncations N. Standard convergence theory is the "horizontal limit", $N \to \infty$ for fixed α. The valley of minimum error in the N-α plane lies along a diagonal limit as marked by the *slanting dashed line* and the *black circles*

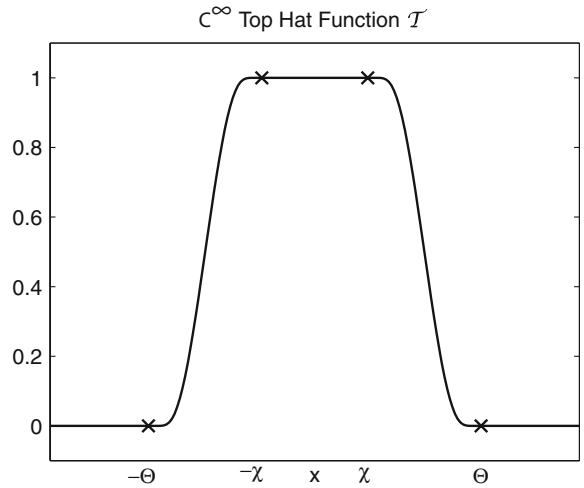

Fig. 4 Schematic of a smoothed, infinitely differentiable top-hat function. The function is "infinitely flat" at the four points marked by x's in the sense that all derivatives of $\mathcal{T}$ are zero at those points, which are also the boundaries of the two smoothing zones

is a function of *two* numerical parameters (N, α) and can therefore be visualized as a contour plot. An N-independent optimum α would imply that the isolines of error are parallel to the α axis and vary only with N—obviously a very special situation, and never observed for Hermite, Laguerre, rational Chebyshev, prolate spheroidal, Gegenbauer and other bases that contain a parameter, in the author's personal experience.

Classical convergence theory is about the *horizontal* limit: it is a description of what happens as $N \to \infty$ for *fixed* α. However, the practical need is to understand and approximate $E(N, \alpha)$ in a *diagonal* limit in which *both* α and N are large as shown schematically in Fig. 3.

This vastening of our conceptualization of convergence must also extend to the asymptotics of spectral coefficients. It is usually easy to calculate the spectral coefficients a_n as $n \to \infty$ with all internal parameters of the basis fixed, and these have some use in applications, but if the asymptotics are to be truly "practical", it is necessary to derive more powerful formulas in which both n and α vary, and the simplifications that ensue from $n \gg \alpha$ are regretfully abandoned.

In what follows, we shall refer to n-and-parameter-both-large asymptotics as "uniform" and the fixed α asymptotics as "non-uniform".

11 Uniform and non-uniform asymptotics for the Fourier coefficients of a C^∞ bell

In applications, it is often convenient to use a "window" or "bell" function which is a smoothed "top hat" function [68,70]. There are many possibilities, but a good window function that is analytic for all real x is

$$\hat{T}(x; L, x_{\text{left}}, x_{\text{right}}) \equiv (1/2)\left\{\text{erf}\left(L(x - x_{\text{left}})\right) - \text{erf}\left(L(x - x_{\text{right}})\right)\right\} \tag{77}$$

where L, x_{left} and x_{right} are user-choosable positive constants. However, $\hat{T}$ is only *approximately* equal to zero for large $|x|$ and approximately equal to one on most of $x \in [x_{\text{left}}, x_{\text{right}}]$. Often, it is desirable to have a "window" of compact support, that is, a function that is identically zero, and not merely approximately zero, outside a finite

interval. One strategy for doing so is to apply a change of coordinates inside the error function so that the argument ranges from $-\infty$ to ∞ while x varies over a finite interval. One such exemplar, which is one on the interval $x \in [-\chi, \chi]$ and zero for $|x| \geq \Theta|$, is:

$$\mathcal{T}(x; L, \chi, \Theta) \equiv \begin{cases} 0, & x \in [-\infty, -\Theta] \\ (1/2)\left(1 + \text{erf}\left\{L \frac{z_{\text{left}}}{\sqrt{1-z_{\text{left}}^2}}\right\}\right), & x \in [-\Theta, \chi] \\ 1, & x \in [-\chi, \chi] \\ (1/2)\left(1 - \text{erf}\left\{L \frac{z_{\text{right}}}{\sqrt{1-z_{\text{right}}^2}}\right\}\right), & x \in [\chi, \Theta] \\ 0, & x \in [\Theta, \infty] \end{cases} \tag{78}$$

where Θ and χ are user-choosable constants with $\Theta > \chi > 0$ and

$$\Omega \equiv (\Theta - \chi)/2 \tag{79}$$

$$z_{\text{left}}(x) = \frac{x - [-\Theta + (\Theta - \chi)/2]}{\Omega} \tag{80}$$

$$z_{\text{right}}(x) = \frac{x - [\Theta - (\Theta - \chi)/2]}{\Omega} \tag{81}$$

This function is illustrated in Fig. 4.

The product

$$\tilde{f}(x) \equiv \mathcal{T}(L, \chi, \Theta)\, f(x) \tag{82}$$

is the sort of beast that is expanded in spectral series in window function applications. The window is optimized by choosing χ so that the interval $x \in [-\chi, \chi]$ includes all of the "physical" domain while $\Theta > \chi$ and L are chosen so that the spectral convergence of $\tilde{f}(x)$ is as rapid as possible. Unfortunately, the convergence of the series for the windowed function $\tilde{f}(x)$ obviously depends strongly on $f(x)$, which it makes it difficult to assert general rules for choosing L and χ.

Instead, the best one can do is to try to understand the asymptotic spectral coefficients when the window is multiplied by a trivial function $f(x) \equiv 1$ or $f(x) \equiv x$ as done in [70]. The rationale is that if a set of parameters is bad for such a trivial multiplier, the rate of convergence of the windowed product $\tilde{f}(x)$ will still be horrible when $\mathcal{T}$ is multiplied by a complicated function with its own internal structure.

In this spirit, Boyd derived both uniform and non-uniform asymptotics for the Fourier coefficients of the periodization of the window (78). To avoid lengthy application-specific details given in [70], suffice it to note that the problem can be reduced, after some transformations, to that of asymptotically evaluating the complex-valued integral

$$I^+(n; L) \equiv \int_{-1}^{1} \exp(\Phi(x)) s(x) \mathrm{d}x, \tag{83}$$

where the rapidly varying phase function is

$$\Phi(x; n, L) \equiv \mathrm{i}nx - L^2x^2/(1 - x^2) \tag{84}$$

and the slowly varying n-independent factor is

$$s(x) \equiv (1 - x^2)^{-3/2}. \tag{85}$$

The integral is the Fourier transform of the symmmetric function of compact support

$$f(x) \equiv \begin{cases} \exp\left(-L^2x^2/(1 - x^2)\right)\ (1 - x^2)^{-3/2}, & |x| \leq 1 \\ 0, & |x| > 1 \end{cases}. \tag{86}$$

(Note that in the original [70], the range of the integral was taken from 0 to 1, which, because of the symmetry of the integrand with respect to $x = 0$, merely halves the integral.)

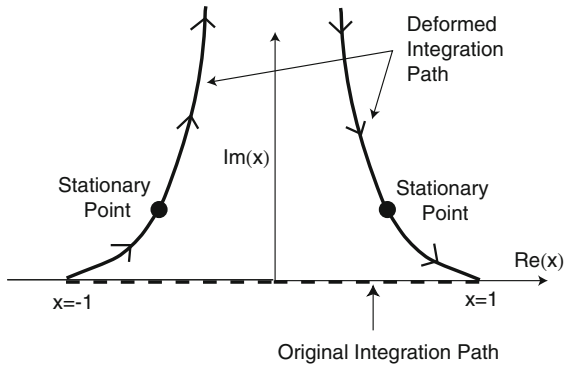

Fig. 5 The original integration path (*dashed*) and the deformed contour of integration (*solid*) of the integral I^+ defined by (83); the path is completed at i∞. The path is symmetric about $\Re\epsilon(x) = 0$ because the integrand is; similarly, the stationary points (*black disks*) are disposed symmetrically with respect to the imaginary axis

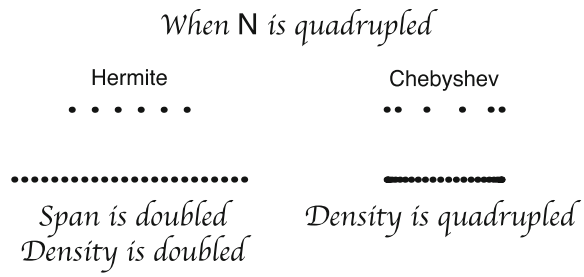

Fig. 6 Schematic of how the Hermite and Chebyshev collocation grids change with N

The next task is to determine the stationary points. The *uniform* asymptotics result from setting

$$L^2 \equiv \lambda n. \tag{87}$$

The phase function is now *linear* in n:

$$\Phi(x; L, n) = n\left\{ \mathrm{i}x - \lambda x^2/(1-x^2) \right\}. \tag{88}$$

The stationary points are the roots of $\mathrm{d}\Phi/\mathrm{d}x$, which after clearing denominators gives the quartic

$$x^4 - 2x^2 + 2\mathrm{i}\lambda x + 1 = 0. \tag{89}$$

There are thus four stationary points, but only the two in the upper half-plane are on the deformed path of integration, which is illustrated in Fig. 5.

It seems to be typical that the uniform asymptotics yield a stationary point equation that can only be solved numerically. Fortunately, it is also typical that the stationary point equation only needs to be solved once for each value of the parameters because it is n-independent. In this case, λ is a free parameter which we wish to choose to give the fastest rate of Fourier convergence or in the language of steepest descents, the largest negative real part of Φ at the stationary point x_s. By plotting $\Phi(x_s)$ versus λ, one finds

$$\lambda = 0.530 \qquad L_{\text{optimum}} = 0.728\sqrt{n}. \tag{90}$$

The usual steepest-descent formula (46) gives

$$I^+(n; \lambda = 0.530) \sim \frac{2}{\sqrt{n}} \exp(-0.354\, n) \times \{-0.336\cos(0.306n) + 1.017\sin(0.306n)\}. \tag{91}$$

When L is *fixed* and independent of n, Φ no longer has n as an overall multiplier and the stationary point is n-dependent. The good news is that it is usually possible, for non-unifom asymptotics, to solve the stationary point equation *perturbatively*. Introducing the parameter

$$\nu \equiv n/L^2 \tag{92}$$

which grows with n, the stationary-point equation becomes

$$\mathrm{i}\nu = \frac{2x}{(1-x^2)^2}. \tag{93}$$

Expanding the location of the stationary point in the upper-right quadrant in inverse powers of ν,

$$x_s \approx 1 - \frac{\exp(-i\pi/4)}{\sqrt{2}} \frac{1}{\sqrt{\nu}} + O(\nu^{-3/2}). \tag{94}$$

Evaluating $\Phi(x_s)$ through a similar expansion yields

$$I^+ \sim \frac{\pi^{1/2}}{L} \exp\left(\frac{3}{4}L^2\right) \exp(-L\sqrt{n}) \left\{\cos(n)\cos\left(L\sqrt{n}\right) + \sin(n)\sin\left(L\sqrt{n}\right)\right\}. \tag{95}$$

In the limit $n \to \infty$ for fixed L, the non-uniform asymptotics show a subgeometric rate of convergence (with also oscillations in degree n) as expected for functions that are infinitely differentiable but not analytic on the expansion interval. The *uniform* asymptotic limit shows a *geometric* rate of convergence, proof of the power of varying the map parameter L with degree n. (The error in truncating a series at $n = N$ is $O(a_N)$ for an exponentially convergent series [1]. Thus, we can optimize the series by choosing an N-dependent L to make the last Fourier coefficient as small as possible.)

The phrase "as small as possible" requires a qualifier because the spectral coefficients are a decaying oscillation in degree n. What actually must be minimized is the exponentially decaying part of a_N, the "envelope" of the spectral coefficients as discussed further in [1] and [70]. One virtue of asymptotic approximations is that they explicitly display the spectral coefficients as the product of a monotonically decaying envelope multiplied by an oscillatory factor.

Boyd [19,31] give other examples where, by varying a parameter in an optimal, n-dependent fashion it is possible to promote subgeometric convergence to a geometric rate of convergence. There are indeed many similarities between the theory of spectral series for C^∞ functions on a finite interval and the theory of spectral series for an unbounded domain as is discussed next.

12 Unbounded interval and C^∞ functions

12.1 Strategies for an unbounded domain

There are three strategies for solving problems on an infinite domain:

1. Apply a finite interval method, such as Chebyshev polynomials, to an interval $x \in [-L, L]$ where L is large but finite ("domain truncation").
2. Map the infinite interval into a finite domain through a change of coordinate and then apply a finite interval method.
3. Use a basis that is intrinsic to the unbounded domain such as Hermite functions.

These options are not mutually exclusive in the sense that the rational Chebyshev functions $TB_n(x; L)$ are an intrinsically infinite-interval basis which was created by a change of coordinate. These same three options apply to the semi-infinite interval except that the relevant basis functions are the rational Chebyshev functions TL_n and TM_n [29,30] and Laguerre functions [30].

However, these options have this in common: All depend either implicitly or explicitly upon a parameter L that allows the scale of the basis functions to be adjusted as closely as possible to the scale of the function $f(x)$ being expanded. Therefore, uniform asymptotics with both the parameter and N large are an important part of the study of infinite and semi-infinite interval methods.

Another complication is that the solutions to engineering or physics problems on an unbounded domain are usually infinitely differentiable on the entire domain but weakly singular at infinity. Many functions can be approximated by inverse power series for large $|x|$; for example, the usual zeroth-order Bessel function is

$$J_0(x) \sim \sqrt{\frac{2}{\pi x}} \left\{\sin(x + \pi/4) \left[1 - \frac{9}{128}\frac{1}{x^2} + \frac{3675}{32768}\frac{1}{x^4} - \cdots\right] - \cos(x + \pi/4)\left[\frac{1}{8}\frac{1}{x} - \frac{75}{1024}\frac{1}{x^3} + \cdots\right]\right\}. \tag{96}$$

In modern software libraries, both power series for small x and inverse power series for large x are usually replaced by Chebyshev series. The crucial point is this: if the inverse series is *asymptotic* but *divergent*, then this implies that the function is C^∞ but not analytic at infinity. The "Chebyshevization" of the inverse power series for the Bessel function, for example, has only a *subgeometric* rate of convergence because the inverse power series they replace are *divergent*.

Another perspective on the ubiquity of C^∞ functions is to observe that if a function $f(x)$ decays proportionally to $\exp(-Ax)$ for some constant A as $x \to \infty$, then the change of coordinate $y = 1/x$ shows $f(x[y])$ has a singularity of the form $\exp(-A/y)$. We have already derived the asymptotic coefficients of a Chebyshev series in y in Sect. 9.2 above.

There is also a purely numerical explanation for why a subgeometric rate of convergence is the norm on an unbounded domain. The collocation points associated with the Hermite basis are the roots of the N-th Hermite function; these are the abcissas of Gaussian quadrature on an infinite interval with the Hermite weight $\exp(-[1/2]x^2)$. From the differential equation satisfied by the Hermite functions, it was shown long ago that the roots are distributed quasi-uniformly on the interval

$$x \in [-\sqrt{2N+1}, \sqrt{2N+1}]. \tag{97}$$

Thus, when N is increased by a factor of four, the span of the grid points in merely doubled. However, the *density* of the grid points (the reciprocal of the spacing between grid points) is also doubled.

When approximating a function $f(x)$ on the fixed interval $x \in [-1, 1]$ by Chebyshev polynomials, the *span* of the grid points remains *fixed* while the density quadruples when N is increased by a factor of four as illustrated in Fig. 6. Why the difference? The answer is that an infinite-interval basis must do "double duty": increasing both the *density* of the grid while simultaneously expanding its *span*.

If a function $f(x)$ is decaying as $\exp(-A|x|)$ as $|x| \to \infty$, then approximating $f(x)$ using domain truncation on a *fixed* interval $x \in [-L, L]$ is a *non-convergent* process because the function is as large as $\exp(-AL)$ at the computational boundaries, and therefore approximating $f(x)$ by zero for $|x| > L$ gives a maximum pointwise error on $x \in [-\infty, \infty]$ of $\exp(-AL)$ even in the limit $N \to \infty$. To apply domain truncation successfully, one must *increase* the domain size L and thereby *increase* the *span* of the grid points as N, the spectral truncation, increases.

This increase-of-span is automatic with Hermite functions (good!). However, the fact that the span of the grid is increasing as $\sqrt{N}$ implies that the *density* of the grid is growing only as $\sqrt{N}$. Since the density of the Chebyshev grid on a fixed interval grows linearly with N, one would expect that the rate of convergence of Hermite series is, in some sense, only the square root of the rate of convergence of a Chebyshev series.

This is in fact exactly the case. Generically, functions $f(x)$ have poles, logarithms and branch points at finite distances from the expansion interval; entire functions which are free of singularities except at infinity, are very special, though the examples of the cosine, sine and exponential show that entire functions are of some importance in applications. For singular functions, the asymptotic rates of decay are [1]

$$\exp(-\mu n), \qquad \text{Chebyshev}, \tag{98}$$

$$\exp(-q\sqrt{n}), \qquad \text{Hermite}. \tag{99}$$

We find indeed that the Chebyshev-to-Hermite change is a replacement of N by its square root. But a decay proportional to the exponential of the square root of n is a subgeometric rate of decay.

12.2 Steepest descent for Hermite coefficients of sub-Gaussian functions

The asymptotic spectral coefficients for domain truncation with Chebyshev polynomials and rational Chebyshev functions are derived in [19] using a mixture of steepest-descent analysis and residue calculus. The Fourier–Cloot–Weideman basis, orthogonal rational functions, Laguerre functions and Hermite expansions for $f(x)$ that decay faster than $\exp(-Ax^2)$ ("super-Gaussians") are similarly analyzed in [62,77,78] and [31], respectively. To illustrate the ideas, however, we shall concentrate on a simple example: Hermite expansions of functions that decay for large x in proportional to $\exp(-A|x|^k)$ for some $k < 2$ ("sub-Gaussian functions") [31].

The n-th normalized Hermite function $\psi_n(x)$ is the product of a Gaussian factor, $\exp(-[1/2]x^2)$, with a polynomial of degree n, the n-th Hermite polynomial. The Hermite functions can be computed easily by

$$\psi_0(x) \equiv \pi^{-1/4} \exp(-(1/2)x^2), \qquad \psi_1(x) \equiv \pi^{-1/4} \sqrt{2}\, x\, \exp(-(1/2)x^2), \tag{100}$$

$$\psi_{n+1}(x) = \sqrt{\frac{2}{n+1}}\, x\, \psi_n(x) - \sqrt{\frac{n}{n+1}}\, \psi_{n-1}(x). \tag{101}$$

However, to evaluate the Hermite coefficients for large n, it is important to have large-n asymptotics for the Hermite functions themselves. Fortunately, these can be obtained by applying the method known variously as "WKB", "JWKB" or the Liouville–Green method to the differential equation ("parabolic cylinder equation") satisfied by the Hermite functions.

The n-th Hermite function *oscillates* on the interval $x \in [-\sqrt{2n+1}, \sqrt{2n+1}]$, and can be approximated by either a sine or cosine on that subdomain, and *decays* exponentially proportional to $x^n \exp(-[1/2]x^2)$ as $|x| \to \infty$. The points

$$x_t \equiv \pm\sqrt{2n+1} \quad \text{["Turning/Stationary Points"]} \tag{102}$$

are called "turning points" because the behavior of the Hermite functions changes from oscillatory to exponential decay at these points. In a neighborhood of either turning point, both the trigonometric and Gaussian asymptotic approximations fail and $\psi_n(x)$ must be approximated by an Airy function.

Because the n-th Hermite function is decaying faster than $f(x)$ when $f(x)$ is "sub-Gaussian" in the sense defined above, the steepest-descent path for the integrals

$$I_1 \equiv \int_{-\infty}^{-\sqrt{2n+1}} \psi_n(x) f(x) \mathrm{d}x, \qquad I_4 \equiv \int_{\sqrt{2n+1}}^{\infty} \psi_n(x) f(x) \mathrm{d}x \tag{103}$$

is along the real axis with the maximum of both integrands at the turning points. Inserting the Airy function approximation,

$$\psi_n(x) \sim \frac{\lambda}{(2n+1)^{1/4}} \mathrm{Ai}(\lambda(x - x_t), \quad \lambda \equiv 2^{1/3}(2n+1)^{1/6}, \tag{104}$$

$$I_1 \sim f(-\sqrt{2n+1}) \int_{-\infty}^{0} \frac{\mathrm{Ai}(-\lambda y)}{(2n+1)^{1/4}} \lambda \mathrm{d}y \sim \frac{f(-\sqrt{2n+1})}{3\,(2n+1)^{1/4}} \tag{105}$$

and similarly for I_4, which is identical except for the substitution at $f(x)$ at the positive turning point for the value of $f(x)$ at the negative turning point. We used $\int_0^\infty \mathrm{Ai}(z)\mathrm{d}z = 1/3$.

To evaluate the Hermite coefficient integral between the turning points, it is convenient to use the decomposition

$$\psi_n(x) = h_n^+(x) + h_n^-(x), \tag{106}$$

where

$$h^{\pm}(x) \sim \frac{\exp(\pm \mathrm{i}\sqrt{2n+1}x)}{2\sqrt{\pi} n^{1/4}}. \tag{107}$$

Watson shows that the $h_n^{\pm}(x)$ have exact expressions as parabolic cylinder functions of complex argument [79] and Hille derives their WKB approximations [80].

The Airy functions grow or decay monotonically along three paths in the complex plane which we shall call "Stokes lines"; these are shown for the local approximations around each turning point in Fig. 7. The function $h_n^+(x)$ decays exponentially as $|x| \to \infty$ along the imaginary axis; the two Airy functions decay along the Stokes lines S_2 and S_5 which eventually merge into the positive imaginary axis beyond the top of the figure. We can thus evaluate the integral of $h_n^+(x) f(x)$ from $-\sqrt{2n+1}$ to $x = \sqrt{2n+1}$ in steepest-descent fashion by deforming the contour of integration to pass from the left turning point to the right turning point by means of the Stokes lines S_2 and S_5. Because

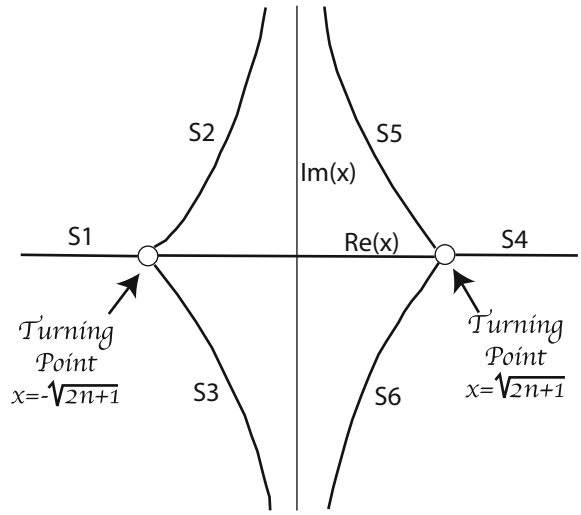

Fig. 7 Stokes lines of the WKB approximation in the complex x-plane, labeled "S1" through "S6"; the Hermite functions $h^{\pm}(x)$ vary exponentially and monotonically along the Stokes lines. The two turning points are marked by circles

$h_n^+(x)$ decays exponentially away from the turning point on the Stokes lines, the contributions again come only from the turning points. When we add the contributions from these integrals together, we finally arrive at the approximation

$$a_n \sim \frac{f(\sqrt{2n+1}) + f(-\sqrt{2n+1})}{(2n+1)^{1/4}} \tag{108}$$

which is (5.15) of [31].

This asymptotic approximation is not restricted to $f(x)$ that decay exponentially. For example,

$$f(x) \equiv 1 = \sum_{m=0}^{\infty} a_{2m}\, \psi_{2m}(x), \tag{109}$$

where

$$a_{2m} = \pi^{1/4}\sqrt{2}\,\frac{\sqrt{(2n)!}}{2^n\, n!} \tag{110}$$

$$\sim 2^{3/4}(2m)^{-1/4}, \qquad m \gg 1, \tag{111}$$

where the asymptotic limit is, upon substituting $n = 2m$, the same as (108).

There is a complication: the deformation of the steepest-descent path is legitimate only if the deformed path does not pass over any poles or branch points of $f(x)$; otherwise, the asymptotic coefficient formula has additional contributions from the residues of the integrand at the poles and similar contributions from branch points. Hille shows that if $f(x)$ has a singularity anywhere along the lines $\Im\mathrm{m}(x) = \pm w$, then the Hermite coefficients will decay proportionally to $\exp(-w\sqrt{2n+1})$ [81], multiplied by a more-slowly varying function of n (such as a power of n) which depends on the type of singularity (pole, logarithm, etc.). If $f(x)$ is an entire function, singular only at infinity, then (108) applies without modification. However, if $f(x)$ is a sub-Gaussian function decaying proportional to $\exp(-A|x|^k)$ for $2 > k > 1$, then the contribution from the singularity will decay more slowly than the stationary-point contribution (108), so the singularity always wins and (108) is irrelevant for sufficiently large n. However, if $k < 1$, then the stationary-point term is decaying more slowly than the singularity term, and thus (108) is asymptotically accurate, even if $f(x)$ has singularities at finite distances from the real axis.

The case $k = 1$ is subtle: if the real axis decay is $\exp(-A|x|)$ and the singularity nearest the real axis is at $|\Im\mathrm{m}(x)| = w$, then (108) is correct as $n \to \infty$ only if $A < w$. This is true for $f(x) = \mathrm{sech}(x)$, for example, for which $A = 1$ and $w = \pi/2$, but its *square*, $f(x) = \mathrm{sech}^2(x)$, is dominated by the singularity because now $A = 2$, which is greater than w, which is still $\pi/2$.

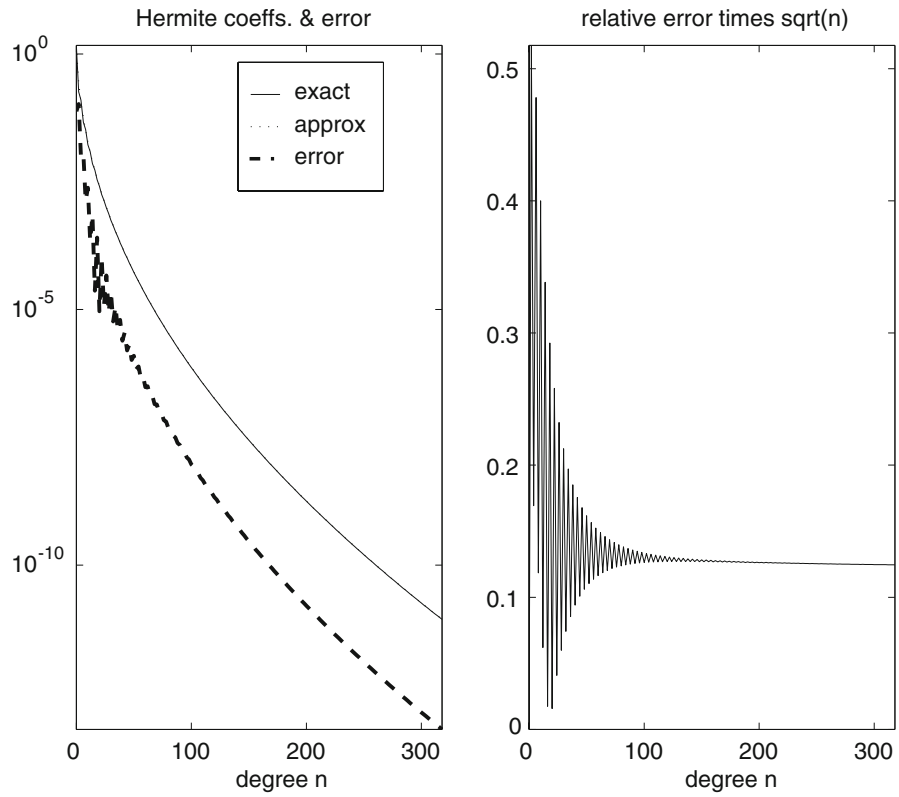

Fig. 8 *Left panel*: the solid and dotted curves, which are graphically indistinguishable, are the exact and approximate normalized Hermite coefficients for $f(x) = \mathrm{sech}(x)$. The *right panel*, which shows the relative error multiplied by $\sqrt{n}$, shows that the relative error asymptotes to approximately $(1/8)/\sqrt{n}$

Figure 8 shows that the approximation (108), which in this case is $a_n^{\mathrm{asy,sech}} \sim 4\exp(-\sqrt{2n+1})/(2n+1)^{1/4}$ for the expansion of $\mathrm{sech}(x)$, is quite accurate for large n. The oscillations in the error for $n < 100$ in the right panel are due to the singularity contribution to a_n, which is completely negligible only for $n > 100$.

A more subtle example is

$$f(x) = \exp(-b(x^2 + a^2)^{k/2}), \tag{112}$$

where $b > 0$ and a are real constants. This asymptotes to $\exp(-b|x|^k)$. When $k < 1$, the stationary-point term dominates. However, there are branch points at $x = \pm \mathrm{i}a$. The contour of integration for the product of $h_n^+(x) f(x)$ between the turning points must be deformed to that shown in Fig. 9. The keyhole-shaped contour around the branch point gives an extra contribution to the asymptotic approximation of the Hermite coefficients. This decays faster than the stationary-point term, but by juggling a and b, we can manipulate the relative importance of these two terms for moderate n.

Figure 10 shows that for the particular combination of parameters $k = 1/2$, $a = 2$ and $b = 10$, the stationary-point approximation (dotted) is way too small for small n. However, the exact and approximate curves merge at about $n = 110$, and the error curve (thick dashes) is about 200 times smaller than the coefficients at $n = 200$. The reason for this "cross-over" is that because b is large (i.e., $f(x)$ has fast spatial decay), the stationary-point contributions to a_n, which are proportional to $f(\sqrt{2n+1})$ are smaller than the branch-point contributions for $n < 110$. It is important to apply asymptotic approximations only asymptotically!

Our last example is apparently a falsification of Darboux's Principle, which asserts that the rate of convergence of a spectral series is completely controlled by its singularities. As noted in Sect. 4, however, the rate of real-axis decay is a statement about the singularity at infinity, so Darboux's Principle is always true. For conceptual purposes,

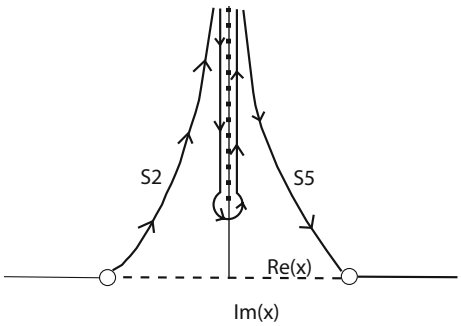

Fig. 9 Thick *solid curves*: new contour of integration for the integral of $h_n^+(x)\,f(x)$ from one turning point (*circle*) to the other. The original contour of integration is dashed; the arrows mark the direction of integration. The cross-hatched line is the branch cut which leads from i∞ to the branch point at $x = ia$

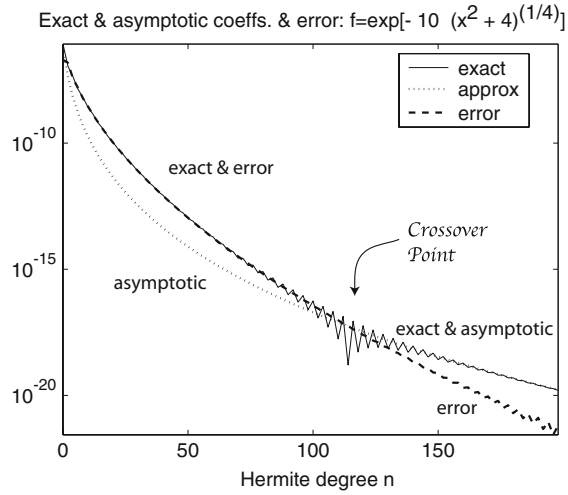

Fig. 10 The *solid* and *dotted curves* are the exact and approximate normalized Hermite coefficients for $f(x) = \exp(-10\sqrt{x^2+4})$. The asymptotic approximation is quite bad for n smaller than the "cross-over" degree, $n \approx 110$, but the error is falling faster than the Hermite coefficients for large n

however, it is useful to make a distinction between the effects of singularities at *finite* locations in the complex x-plane and the effect of the singularity at infinity, which is most easily characterized by the rate of decay of $f(x)$ on the real axis as $|x| \to \infty$.

13 Prolate spheroidal functions

The prolate spheroidal functions of order zero, which depend upon a parameter c called the bandwidth, are generalizations of the Legendre polynomials, which are the special case $c = 0$. Xiao et al. [82] pointed out that the prolate functions oscillate more uniformly over the interval $x \in [-1, 1]$ than the Legendre polynomials and therefore give better accuracy in at least some circumstances. Because the prolate functions are orthogonal with the same weight and interval as the Legendre polynomials, it is trivial to substitute prolate for Legendre in a spectral element code. Their work has inspired both numerical [49,83,84] studies and applications [85–87].

It is important to choose the bandwidth c wisely—too small, and the prolate basis is just a complicated way to apply Legendre polynomials; too large, and the prolate basis is *worse* than the Legendre polynomials. Unfortunately, the theory of asymptotic coefficients for prolate series is in a very bad state. Boyd has done some interesting numerical experiments [49], but because the prolate functions are known only as Legendre series and rather complicated asymptotic approximations, analytic progress has been almost nonexistent. This is very unfortunate because the full potential of the prolate basis can only be realized when the relationship between the asymptotic Legendre and prolate coefficients, the latter as a function of both degree n and the bandwidth parameter c, is well understood. Indeed, it is not an exaggeration to say that the main obstacle to much more widespread application of prolate functions is the poor state of prolate asymptotic coefficient theory.

14 Singularity structures and fractal geometry

To date, the asymptotic theory of spectral coefficients has been mostly restricted to the expansions of functions $f(x)$ that have only simple isolated singularities like poles and branch points in the complex x-plane. However, it is known

that $f(x)$ that solve nonlinear differential equations in applications may have very complicated singularity structures.

For example, the Blasius function, which solves a classic problem in fluid mechanics posed by H. Blasius in 1908, has three singularities of identical form at a distance $S = 5.69004$ from the origin which limit the convergence of the power series about $x = 0$; one is on the negative real axis and the other two are at angles of ± 60 degrees relative to the postive real axis. Their form is [88]:

$$\begin{aligned} f \approx & \frac{6}{x-S} - 1.5036(1+x/S)\cos(\sqrt{2}\log(1+x/S) + 0.54454) \\ & + (1+x/S)^3\left(-0.1152\cos(\sqrt{8}\log\left(1+\frac{x}{S}\right) + 1.0891)\right. \\ & \left. + 0.021323\sin(\sqrt{8}\log\left(1+\frac{x}{S}\right) + 1.0891) + 0.2144\right) + \cdots . \end{aligned} \tag{113}$$

The leading singularity is a simple pole, and thus the leading-order asymptotic approximation to the spectral coefficients, either power series or the rational Chebyshev series on $x \in [0, \infty]$ [88], can be calculated easily. However, the asymptotic form of the coefficients for a function with a cos-of-logarithm singularity is unknown, even for ordinary power series, never mind Chebyshev or Fourier series.

Boyd [88] shows that the Blasius function has an infinite number of other singularities, forming a complicated pattern within three symmetric wedges in the complex plane, but these singularities are all isolated. However, it seems to be quite common for singularities to cluster so densely so as to form a so-called "natural boundary" in the complex plane such that $f(x)$ cannot be analytically continued beyond the boundary. Even more surprisingly, these natural boundaries often have a *fractal* geometry: that is, the boundary curves have increasingly fine structure at increasingly fine scales so that the perimeter of the boundary is *infinite* within a portion of the complex plane bounded by say $\Re\mathfrak{e}(x) = \pm 1$ even though the natural boundary encloses only a finite area within $|\Re\mathfrak{e}(x)| \leq 1$ [89–92].

It is known that spectral series apparently have no difficulties with such functions; if no part of the singularity structure touches the real axis, the spectral series will converge exponentially fast. However, for the coefficients of $f(x)$ with natural boundaries, asymptotic approximations as $n \to \infty$ are a mystery. Huang and Strichartz [93] review some pioneering efforts, but these are no more than a beginning.

15 Two-dimensional spectral-coefficient asymptotics

15.1 Introduction

Two-dimensional convergence theory, even when the basis functions are direct products of one-dimensional sets, is much more subtle than its one-dimensional counterpart. The first difficulty is that coordinate y acts as a parameter for the convergence of the basis functions in the other coordinate x, and therefore the rates and regions of convergence can be very intricate. The second is that multidimensional spectral series may converge badly and display Gibbs' Phenomenon even at points where the function is analytic, and the decay of spectral coefficients may be highly anisotropic. The third complication is that, even in the plane, one must distinguish between "point", "line", "corner" and "spiral" singularities, and more intricate pathologies arise in higher dimensions.

Nevertheless, it is still possible to derive asymptotic approximations to Fourier transforms and spectral series. Indeed, these asymptotics are essential in understanding some of these multidimensional complications.

16 Coordinate interference

"Coordinate interference effects" are illustrated by the function

$$\lambda(x,y) \equiv \frac{1-p(y)^2}{(1+p(y)^2) - 2p(y)\cos(x)} = 1 + 2\sum_{m=1}^{\infty} p(y)^m \cos(mx). \tag{114}$$

The series in x converges geometrically with each term smaller than its predecessor by a factor of p—but if $p(y)$ is a function of y, then the rate of convergence in x is a function of y, too. If, for example, $p(y) = s\cos(y)$ where s is a constant smaller than one, then

$$\lambda(x, y) = \sum_{m=0}^{\infty} \sum_{n=0}^{\infty} a_{mn} \cos(mx)\cos(ny), \tag{115}$$

where a_{mn}=0 for all $n > m$ because $p(y)^m$ is a trigonometric polynomial of degree m in y. Thus, there is geometric convergence in x, but a finite, terminating series in y. The number of terms in the x-degree m to reach a given error tolerance is strongly dependent on the other coordinate y.

In one dimension, each type of spectral series converges in the complex plane within a domain bounded in the x-plane—the interior of a circle for a Taylor series, the interior of an ellipse for Chebyshev and Legendre series and so on. In multiple dimensions, the regions of convergence are very complicated, even for the simplest case of ordinary power series. The Taylor series of $1/(1 - xy)$, for example, converges within the cross-shaped region $|x||y| < 1$ in the four-dimensional space of two complex variables.

Nevertheless, it is possible to prove theorems closely analogous to their one-dimensional contourparts. Integration-by-parts, for example, yields the following theorem in any number of dimensions.

Theorem 9 (Fourier beyond-all-orders rate of convergence) *If f is infinitely differentiable and periodic on the d-dimensional torus, then for any N, there exists a constant A such that*

$$|a_{m1,m2,\ldots,md}| \le \frac{A}{\left(1 + \sqrt{m_1^2 + m_2^2 + \cdots m_d^2}\right)^N} \tag{116}$$

for all $\vec{m}$ where $\vec{m} = m_1, m_2, \ldots, m_d$ and the m_j range over all the integers and

$$f(\vec{x}) = \sum_{\vec{m}=-\infty}^{\infty} a_{\vec{m}} \exp(i\vec{m} \cdot \vec{x}), \tag{117}$$

[94, p. 3, Theorem 2.2].

There is a multi-dimensional Fourier Asymptotic Coefficient Expansion [95], but this is so similar to its one-dimensional counterpart that the details are omitted.

Theorem 10 (Box geometric convergence theorem) *If a function $f(x, y)$ is periodic in two space dimensions with period 2π and is free of singularities everywhere inside the four-dimensional strip, $\mathfrak{Re}(x), \mathfrak{Re}(y)$ equals anything, $|\mathfrak{Im}(x)| \le \mu_1$ and $|\mathfrak{Im}(y)| \le \mu_2$, then the Fourier series converges everywhere within this domain in the complex $x - y$ plane and furthermore*

$$|a_{mn}| \le \textit{constant}\ \exp(-\mu_1|m| - \mu_2|n|), \quad \forall m, n. \tag{118}$$

Proof Make the change of variable

$$x = X \pm \mathrm{i}\tilde{\mu_1}, \qquad y = Y \pm \mathrm{i}\tilde{\mu_2}, \tag{119}$$

where we will try in turn all four possible combinations of signs and $\tilde{\mu}_1 \equiv \mu_1 - \epsilon$ where ϵ is an arbitrarily small positive constant and define

$$g(X, Y) \equiv f(X \pm \mathrm{i}\mu_1, Y \pm \mathrm{i}\mu_2) = \sum_{m=-\infty}^{\infty} \sum_{n=-\infty}^{\infty} b_{mn} \exp(\mathrm{i}mX + \mathrm{i}nY), \tag{120}$$

where

$$b_{mn} \equiv a_{mn} \exp(\pm m\tilde{\mu}_1 \pm n\tilde{\mu}_2]). \tag{121}$$

Now $g(X, Y)$ is analytic and periodic for real X and Y because of our assumption that $f(x, y)$ is analytic in (x, y) even at a distance μ_1 and μ_2 from the real x and y axes. The Fourier Beyond-All-Orders Convergence Theorem above shows that the coefficients b_{mn} must fall faster than any finite inverse power of m and n. However, the coefficients b_{mn} are exponentially growing relative to those of a_{mn} in one of the four sectors of the $m - n$ plane; by considering four different transformations of (x, y) to (X, Y), we can find a set of b_{mn} that is growing relative to a_{mn} in each of the four sectors of the $m - n$ plane. It follows that the a_{mn} must decay exponentially fast with both $|m|$ and $|n|$ as claimed in the theorem, or otherwise the b_{mn} would diverge. □

Similarly, Bochner and Martin [96] prove the following theorem (pp. 94–95), using non-standard notation in which their functions R_j are twice the usual Chebyshev polynomials.

Theorem 11 (Multidimensional Chebyshev series) *Let z_j, $j = 1, 2, \ldots, d$ each denote an ordinary complex variable and let $f(z_1, z_2, \ldots, z_d)$be analytic in the elliptic polycylinder*

$$\mathcal{E} = \left\{ \left| z_j + \sqrt{z_j^2 + 1} \right| < r_j, \;\; j = 1, 2, \ldots, d \right\}, \tag{122}$$

where $r_j > 1$, $j = 1, 2, \ldots, n$. Then $f(z_1, z_2, \ldots, z_d)$ has the unique expansion

$$f(z_1, z_2, \ldots, z_d) = \sum_{j_1=0}^{\infty} \sum_{j_2=0}^{\infty} \cdots \sum_{j_d=0}^{\infty} a_{j_1, j_2, \ldots, j_d} \, T_{j_1}(z_1) \, T_{j_2}(z_2) \ldots T_{j_d}(z_d) \tag{123}$$

valid in $\mathcal{E}$. Convergence is uniform and absolute in every interior polycylinder $E(\rho_1, \ldots, \rho_j)$ for which $1 < \rho_j < r_j$, $j = 1, 2, \ldots, d$.

The coefficients satisfy the bound

$$|a_{j_1, j_2, \ldots, j_d}| \le K(\rho) \frac{1}{\rho_1^{j_1}} \frac{1}{\rho_2^{j_2}} \cdots \frac{1}{\rho_d^{j_d}}, \qquad j_1 = 0, 1, \ldots, j_2 = 0, 1, \ldots, j_d = 0, 1, \ldots. \tag{124}$$

If $f(z)$ is analytic in the union of two polycylinders $E(r_1', \ldots, r_d')$, $E(r_1'', \ldots, r_n'')$, then this function can be continued into the union of all polycylinders $E(r_1, \ldots, r_d)$ where

$$\log\left(r_j\right) = \theta \, \log(r_j') + (1 - \theta) \, \log(r_j''), \qquad 0 \le \theta \le 1, \tag{125}$$

[96, pp. 94–95].

Note that $E(r) = \{|z + \sqrt{z^2 + 1}| < r\}$ is an ellipse with foci at ± 1 with r as the sum of the semimajor axis and the semiminor axis.

In one dimension, the ellipse that appears in the theorem is precisely the domain of convergence in the complex plane. In multiple dimensions, the theorem guarantees convergence within the "polycylinder" which is the multidimensional generalization of an ellipse, but the series almost certainly converges in some parts of the multidimensional complex domain *outside* the polycylinder of guaranteed convergence.

17 Complexities of Gibbs' phenomenon and coefficient decays in multiple dimensions

Gray and Pinsky [97,98] have shown that in three-dimensional spherical coordinates, the Bessel–Fourier series of a step function in radius, discontinuous only at $r = 1$, *diverges* at $r = 0$, even though the function is smooth there; this is now called the "Pinsky Phenomenon". This is but one of many details that have prompted much recent work on the multidimensional Gibbs phenomenon [99–107].

Most of this work has focused on the asymptotics of the Fourier Transform of the "characteristic" or "indicator" function of a region $\mathcal{B}$, which is a function that is equal to one everywhere on the interior of the region and then is zero everywhere else. The "characteristic" function thus has a jump discontinuity of unit magnitude everywhere on the boundary of the region $\partial\Omega$. Helmberg [103] shows that if this function is multiplied by a smoothly varying function

so that the magnitude of the jump smoothly varies on $\partial\mathcal{B}$, this has no significant effect on the Gibbs Phenomenon except for the obvious one that the oscillations locally scale with the jump; this is discussed further below.

If the characteristic function of $\mathcal{B}$ is periodized into a spatially periodic function, then, with the implicit assumption that $\mathcal{B}$ is always smaller than the period box, the multidimensional Poisson Summation shows that the Fourier coefficient $a_{mn} = a(m, n)$ is just the Fourier Transform of the characteristic function. Thus, these studies on the asymptotics of the transform are (implicitly) studies of the Fourier coefficients of a periodic function with jumps.

To classify the phenomenology of Fourier series, it is helpful to write the wavenumber vector (m, n) in polar coordinates as

$$m = \kappa\cos(\eta), \qquad n = \kappa\sin(\eta) \tag{126}$$

and also to define the following.

Definition 5 (*circular and square truncations*) A Fourier series is said to have a circular truncation of degree N if the sum is restricted to those wavenumbers such that

$$\sqrt{m^2 + n^2} = \kappa \le N/2 \tag{127}$$

and a square truncation of degree N if restricted to

$$|m| \le N/2 \qquad \& \qquad |n| \le N/2, \tag{128}$$

that is, a total of approximately N^2 terms.

The most important findings are the following:

1. If $\partial\mathcal{B}$ is smooth, then writing (m, n) in polar coordinates (κ, η), the Fourier coefficients/transform of the characteristic function decay as $\kappa^{-3/2}$ in two dimensions.
2. Under the same conditions with either a circular or square truncation of degree N, the error at a generic point (x, y) falls inversely linearly, that is, denoting the truncated Fourier series by $f_N(x, y)$,
$$|f(x, y) - f_N(x, y)| \le \text{constant}/N \tag{129}$$
3. However, if the point is allowed to move closer to the discontinuity as N increases, the error will converge to a constant, just as in one space dimension. More precisely, if (x_0, y_0) is a point on $\partial\mathcal{B}$
$$\lim_{N\to\infty} |f_N([x - x_0]/N, [y - y_0]/N)| \neq 0 \tag{130}$$
4. If the discontinuity curve $\partial\mathcal{B}$ is non-smooth because of corners, such as when $\mathcal{B}$ is a polygon, then the Fourier coefficients/transform may be highly nonistropic, decaying as fast as $O(1/\kappa^2)$ in some directions in the $m-n$ plane but as slowly as $O(1/\kappa)$ in others. The other propositions are unaltered by the presence or absence of corners in $\partial\mathcal{B}$.

The error decays more slowly than the coefficients, falling as $O(1/N)$ even though the smallest coefficients are typically $O(1/N^{3/2})$, because many coefficients of this magnitude are neglected in the truncation.

To illustrate these assertions about the rate of coefficient decay, it is useful to consider a couple of examples. If the curve of discontinuity is a circle of radius R, then the periodized function is, implicitly restricting $R < \pi$, [106]

$$\frac{R}{2\pi}\sum_{k=-\infty}^{\infty}\sum_{m=-\infty}^{\infty}\frac{1}{\sqrt{m^2+n^2}}J_1\left(\sqrt{m^2+n^2}R\right)\exp\left(\mathrm{i}[kx+my]\right)$$
$$= \sum_{m=-\infty}^{\infty}\sum_{n=-\infty}^{\infty} P\left(\sqrt{(x-2\pi m)^2+(y-2\pi n)^2}\right), \tag{131}$$

where the pattern function is

$$P(r) \equiv \begin{cases} 1, & r < R \\ 0, & r > R \end{cases} \tag{132}$$

and the Fourier coefficients are, abbreviating $\kappa = \sqrt{m^2 + n^2}$,

$$a_{mn} = \frac{R}{2\pi}\frac{1}{\kappa} J_1(\kappa R) \tag{133}$$

$$\sim \frac{\sqrt{R}}{\sqrt{2}\pi^{3/2}}\frac{1}{\kappa^{3/2}} \cos(\kappa R - (3/4)\pi), \qquad \kappa \gg 1, \tag{134}$$

where we have applied the usual asymptotic formula for the Bessel functions in the last line. Thus, the Fourier coefficients decay isotropically as $\kappa^{-3/2}$ for a jump along a circular boundary, as predicted for any smooth curve of discontinuity location.

In contrast, suppose $f_{\text{square}}(x, y)$ is the periodization of the characteristic function of a square:

$$f_{\text{square}}(x, y) \equiv \begin{cases} 1, & |x| < S \text{ and } |y| < S \\ 0, & \text{otherwise} \end{cases} \tag{135}$$

$$= \sum_{m=-\infty}^{\infty} \sum_{n=-\infty}^{\infty} a(m, n) \exp(\mathrm{i}mx + iny), \tag{136}$$

where

$$a(m, n; S) = \frac{1}{4\pi^2} \int_{-S}^{S} \int_{-S}^{S} \mathrm{d}x\mathrm{d}y \exp(-\mathrm{i}mx - \mathrm{i}ny) \tag{137}$$

$$= \frac{1}{\pi^2}\frac{1}{nm} \{\sin(mS) \sin(nS)\} \tag{138}$$

$$= \frac{2}{\pi^2}\frac{1}{\kappa^2 \sin(2\eta)} \{\sin(S\kappa \cos(\eta)) \sin(S\kappa \sin(\eta))\}. \tag{139}$$

In most directions in the wavenumber plane, a_{mn} decays as $O(1/\kappa^2)$. However, if $|\eta - p(\pi/2)| \ll 1/\kappa$ for any integer p, then

$$a(S\kappa \cos(\eta), S\kappa \sin(\eta)) \approx \frac{S}{\pi^2}\frac{\sin(S\kappa)}{\kappa}, \tag{140}$$

which is an $O(1/\kappa)$ decay.

When the Fourier series are summed, however, most of the distinction between jump-at-circle and jump-at-square is washed away. In either case, the error decays as $1/N$ where N is the truncation. Figure 11 shows that the patterns of errors are rather similar even though the coefficients are strikingly different.

Figure 12, which is a blow-up of just the error for the square, shows that there is an interesting phenomenology to the Fourier errors in multiple dimensions. In particular the errors are highly anisotropic in the $x - y$-plane, decaying much faster along the diagonal $y = x$ than along either of the coordinate axes, for both discontinuity curves with corners and discontinuity curves without corners.

Anisotropies in the wavenumber plane can be masked by taking "spherical means", which in two dimensions are really "cylindrical means":

$$a_{\text{mean}}(\kappa) \equiv \sqrt{\int_0^{2\pi} a(\kappa \cos(\eta), \kappa \sin(\eta))^2 \, \mathrm{d}\eta}. \tag{141}$$

Podkorytov's theorem [100,108] shows that, regardless of whether $\partial\mathcal{B}$ has corners or not,

$$a_{\text{mean}}(\kappa) \leq \text{constant}\, \kappa^{-3/2}. \tag{142}$$

Nevertheless, there are subtleties in the error besides the anisotropy visible in Fig. 12. Popov asserts that for the characteristic function of an ellipse, for example, the error decays only as $N^{-5/6}$ on the "evolute" of the ellipse, that is, on the curve which is the envelope of the centers of curvature of the ellipse, and the rate further slows to $N^{-3/4}$ at the four points which are the singularities of the evolute. Figure 13 shows a typical ellipse with its evolute.

A plot of the spatial errors for sufficiently large truncation N should therefore clearly show the evolute with spikes of large error adorning the tips of each point of the four-armed "astroid". However, calculations at resolutions as

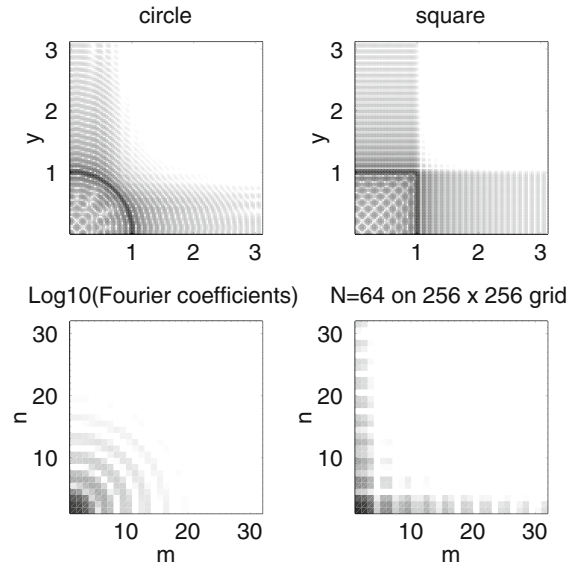

Fig. 11 *Left*: $\log_{10}$ errors in the $x - y$ plane for the circle (top) and Fourier coefficients $|a_{mn}|$ in the m-n plane (bottom) for the characteristic function of a disk (marked by the black circle of $O(1)$ error in the top left graph.) *Right*: same but for the function $f_{\text{square}}(x, y)$ which is discontinuous on a square

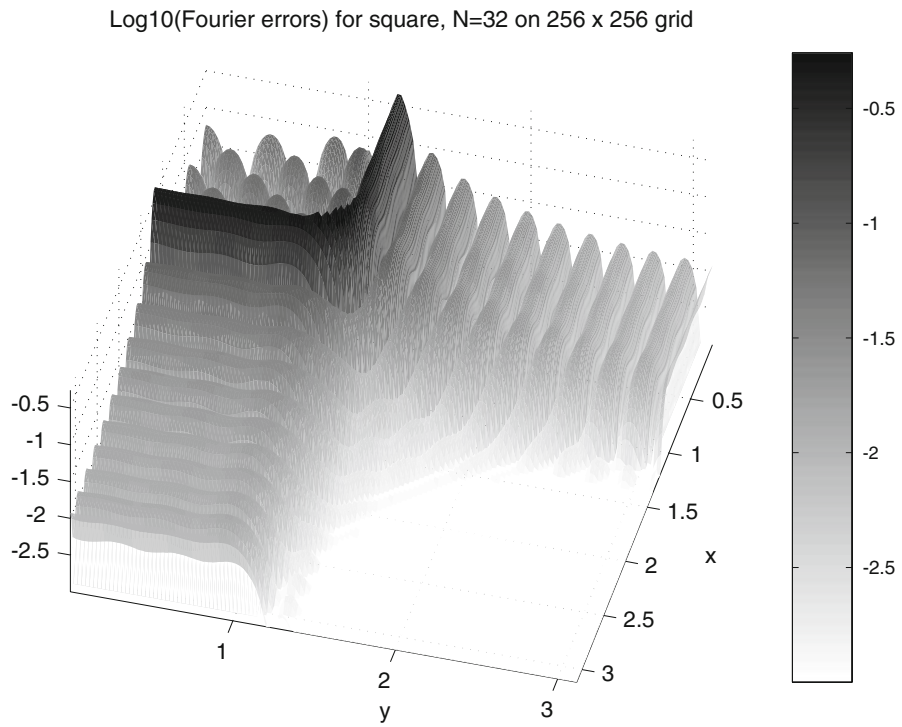

Fig. 12 $\log_{10}$(error) of the Fourier series whose coefficients a_{mn} are truncated to $|m|, |n| < 16$ as plotted in the $x - y$-plane for a function which is equal to one on the unit square and is zero elsewhere in the basic period box, $x \in [-\pi, \pi]$, $y \in [-\pi, \pi]$. Because both the function $f(x, y)$ and errors are symmetric with respect to the both the x- and y-axes, only one quadrant of the period box is illustrated. For clarity, a floor of 0.001 is applied (white area on the plot)

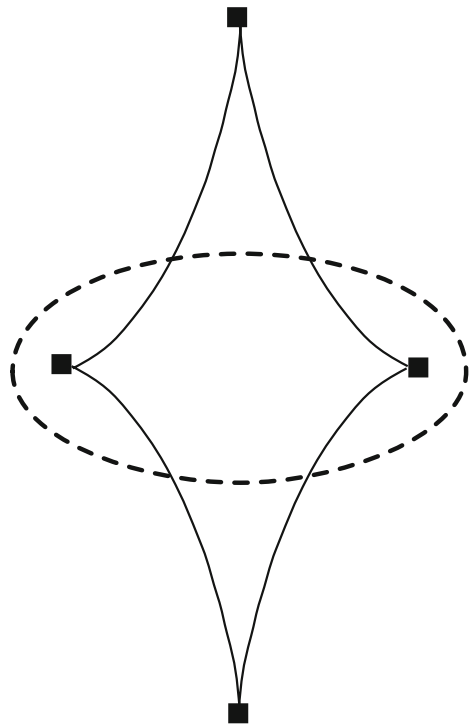

Fig. 13 Schematic of an ellipse (*dashed*) and its evolute (*solid*; a curve known as an "astroid") and its four singularities [*small black squares*]

high as 4096×4096 show no hint of unusually large error on the evolute; no graph is shown because there is literally nothing to show except a large, thin ridge of $O(1)$ error around the ellipse itself, even with a logarithmic error scale.

It is perhaps appropriate in a special issue on "Practical Asymptotics" to sometimes encounter "impractical asymptotics" in the sense that subtle differences due to fractional powers of N are apparent only at much larger N than can ever be graphed on a computer screen with its limited resolution of at most 2000×2000 pixels. The existing error bounds and asymptotic coefficient bounds give a broad picture, but precise asymptotics, complete with proportionality constants, and a dictionary of the relationship between curves and coefficients—this pattern for $\partial\mathcal{B}$ a hexagon, this pattern of coefficients when the discontinuity curve is the ovals of Cassini—is still lacking.

18 Poisson summation and imbricate series in two dimensions

The Poisson summation theorem is valid in an arbitrary number of dimensions, but for simplicity, we shall state only the two-dimensional version.

Theorem 12 (Poisson summation/imbricate series 2D) *Let $a(k, m)$ and $P(x, y)$ be a Fourier transform pair defined by*

$$a(m, n) \equiv \frac{1}{4\pi^2} \int_{-\infty}^{\infty} \int_{-\infty}^{\infty} P(x, y)\ \exp(-\mathrm{i}(kx + my))\mathrm{d}x\mathrm{d}y, \tag{143}$$

$$P(x, y) \equiv \int_{-\infty}^{\infty} \int_{-\infty}^{\infty} a(m, n)\ \exp(\mathrm{i}(mx + ny))\mathrm{d}m\,\mathrm{d}n. \tag{144}$$

Let a function $u(x, y)$ be defined by employing $a(k, m)$ as its Fourier coefficients. Then $u(x, y)$ can be written as either of the two alternative series

$$u(x, y) = \sum_{k=-\infty}^{\infty} \sum_{m=-\infty}^{\infty} a(m, n)\ \exp(\mathrm{i}(mx + ny)) \tag{145}$$

$$= \sum_{m=-\infty}^{\infty} \sum_{n=-\infty}^{\infty} P(x - 2\pi m, y - 2\pi n), \tag{146}$$

where the top series is the usual Fourier expansion and the bottom sum is the imbricate series with $P(x, y)$ as the pattern function.

18.1 Fourier transforms in polar coordinates

It is easiest to construct examples of two-dimensional periodic functions by using a radially-symmetric pattern function. This makes the following useful.

Let $\vec{k}$ denote the wavevector whose components are (m, n) and $\vec{x}$ the position vector with components (x, y). Define polar coordinates for both wavevector and physical space via

$$(m, n) \equiv (\kappa\ \cos(\eta),\ \kappa\ \sin(\eta)), \tag{147}$$

$$(x, y) \equiv (r\ \cos(\phi),\ r\ \sin(\phi)). \tag{148}$$

Theorem 13 (Fourier transforms in polar coordinates)

$$a(\kappa, \eta) \equiv \frac{1}{4\pi^2} \int_0^{\infty} r\,\mathrm{d}r \int_{-\pi}^{\pi} \mathrm{d}\phi\ P(r, \phi)\ \exp(-\mathrm{i}\kappa\ r\ \cos[\phi - \eta]), \tag{149}$$

$$P(r, \phi) \equiv \int_0^{\infty} \kappa\,\mathrm{d}\kappa \int_{-\pi}^{\pi} \mathrm{d}\eta\, a(\kappa, \eta)\ \exp(\mathrm{i}\kappa\ r\ \cos[\phi - \eta]). \tag{150}$$

If the coefficient function $a(\kappa, \eta)$ and pattern function $P(r, \phi)$ have the Fourier expansions

$$a(\kappa, \eta) = \alpha_0(\kappa) + \sum_{n=1}^{\infty} \alpha_n(\kappa)\ \cos(n\eta) + \beta_n(\kappa)\ \sin(n\eta), \tag{151}$$

$$P(r, \phi) = p_0(r) + \sum_{n=1}^{\infty} p_n(r)\ \cos(n\phi + q_n(r)\ \sin(n\phi), \tag{152}$$

the coefficients are related by

$$\alpha_n(\kappa) = \frac{(-\mathrm{i})^n}{2\pi} \int_0^{\infty} J_n(\kappa r)\ p_n(r)\, r\,\mathrm{d}r, \qquad n = 0, 1, 2, \ldots, \tag{153}$$

$$\beta_n(\kappa) = \frac{(-\mathrm{i})^n}{2\pi} \int_0^{\infty} J_n(\kappa r)\, q_n(r)\, r\,\mathrm{d}r, \qquad n = 1, 2, \ldots, \tag{154}$$

$$p_n(r) = 2\pi\ \mathrm{i}^n \int_0^{\infty} J_n(\kappa r)\, \alpha_n(\kappa)\, \kappa\,\mathrm{d}\kappa, \qquad n = 0, 1, 2, \ldots, \tag{155}$$

$$q_n(r) = 2\pi\ \mathrm{i}^n \int_0^{\infty} J_n(\kappa r)\, \beta_n(\kappa)\, \kappa\,\mathrm{d}\kappa, \qquad n = 0, 1, 2, \ldots. \tag{156}$$

For the special case of a radially symmetric pattern:

$$\alpha(\kappa) = \frac{1}{2\pi} \int_0^{\infty} J_0(\kappa r)\ P(r)\, r\,\mathrm{d}r, \tag{157}$$

$$P(r) = 2\pi \int_0^{\infty} J_0(\kappa r)\, \alpha(\kappa)\, \kappa\,\mathrm{d}\kappa. \tag{158}$$

19 Point versus curve singularities

The third complication of multiple dimensions is that a function of two variables may be singular along a *curve* in the $x - y$ plane, which we shall dub a "curve" singularity or only at a single point, which we shall dub a "point" singularity. Limited experience indicates that a point singularity of a given type, such as a discontinous slope, has a less deleterious effect on spectral convergence than a singularity on a curve of finite length.

The Poisson Summation theory makes it easy to generate examples. A slope discontinuity at the origin may be dubbed a "cone singularity" since $f_{\text{cone}}(x, y)$ has locally the shape of a cone. An example of a cone singularity with a radially symmetric pattern function is

$$P(r) \equiv \begin{cases} (R-r)^2, & r \le R \\ 0, & r > R \end{cases}. \tag{159}$$

The Fourier coefficient function $a(k, m) = \alpha(\sqrt{k^2 + m^2})$ is

$$\alpha(\kappa) = \frac{1}{2\pi} \int_0^R J_0(\kappa r)\,(R-r)^2\, r\,\mathrm{d}r \tag{160}$$

$$= \frac{R^2}{2\pi\kappa^2} \left\{ 2J_0(R\kappa) - 4\frac{J_1(R\kappa)}{R\kappa} - \pi J_0(R\kappa)\mathbf{H}_1(R\kappa) - \pi J_1(R\kappa)\,\mathbf{H}_0(R\kappa) \right\}$$

$$\sim \frac{R}{\pi\,\kappa^3} + O(\kappa^{-7/2}). \tag{161}$$

where $\mathbf{H}_0$ and $\mathbf{H}_1$ are usual Struve functions [109] and the $O(\kappa^{-7/2})$ term arises because there is a second derivative discontinuity at $r = R$.

A function with a slope discontinuity on the circle $R = a$ and a radially-symmetric pattern function is

$$P(r) \equiv \begin{cases} R^2 - r^2, & r \le R \\ 0, & r > R \end{cases}, \tag{162}$$

which implies

$$\alpha(\kappa) = \frac{1}{2\pi} \int_0^R J_0(\kappa r)(rR^2 - r^3)\,\mathrm{d}r \tag{163}$$

$$= \frac{2R}{\pi}\,\frac{J_1(R\kappa)}{\kappa^3} - \frac{R^2}{\pi}\frac{J_0(R\kappa)}{\kappa^2} \sim -\sqrt{2}\frac{R^{3/2}}{\pi^{3/2}}\frac{\sin(R\kappa + \pi/4)}{\kappa^{5/2}}. \tag{164}$$

The point singularity is weaker than the curve singularity in the sense that the curve singularity gives Fourier coefficients decaying as $O(\kappa^{-5/2})$ whereas those of the cone function decay as $O(\kappa^{-3})$.

Integration-by-parts, applied to the multidimensional Fourier coefficient integral, shows that each additional bounded derivative increases the order of convergence by one power of $\kappa \equiv \sqrt{m^2 + n^2}$; the argument is to integrate-by-parts until further integrations would yield a singular integral; one can then bound the surface terms and the integral to show that the coefficients are bounded by a power of κ as the wavenumbers (m, n) tend to infinity. This argument is so similar to the one-dimensional case that we omit details.

Instead, we note that examples make the same point in more explicit and concrete fashion. For example, the pattern function

$$P(r) \equiv \begin{cases} R^2/6 + r^3/(3R) - r^2/2, & r \le R \\ 0, & r > R \end{cases} \tag{165}$$

Table 2 Singularities and coefficient convergence for two-dimensional Fourier series

Singularity type	Fourier coefficients decay as
Curve singularities	
Discontinuity at a circle	$\kappa^{-3/2}$
First derivative discontinuous at a circle	$\kappa^{-5/2}$
Second derivative discontinuous at a circle	$\kappa^{-7/2}$
Point singularities	
Logarithmic singularity at the origin	κ^{-2}
Cone singularity (first derivative)	κ^{-3}
$r^2\log(r)$ at $r=0$	κ^{-4}
Discontinuous third derivative at $r=0$	κ^{-5}
$r^4\log(r)$ at $r=0$	κ^{-6}

Note: κ is the magnitude of the vector whose components are (m, n), the Fourier degrees in x and y, respectively. A circle of discontinuity can be replaced by any smooth curve.

has a discontinous *second* derivative on the circle $r = R$, but P and all its first derivatives are continuous everywhere. The Fourier coefficient function is

$$\alpha(\kappa) = \frac{1}{2\pi}\int_0^R J_0(\kappa\, r)\ \left(R^2/6 + r^3/(3R) - r^2/2\right)\,\mathrm{d}r \tag{166}$$

$$= \frac{3J_1(R\kappa)\mathbf{H}_0(R\kappa)}{4\kappa^4} - \frac{3J_0(R\kappa)\mathbf{H}_1(R\kappa)}{4\kappa^4} - \frac{R\,J_1(R\kappa)}{2\pi\,\kappa^3}$$

$$\sim \frac{\sqrt{R}\cos(R\kappa + \pi/4)}{\pi^{3/2}\sqrt{2}\,\kappa^{7/2}} + O(\kappa^{-9/2}). \tag{167}$$

Comparing this example with (133) and (163) allows us to make the first three entries in Table 2.

Similarly, a logarithmic point singularity example is

$$P(r; a) = K_0(ar) \to \alpha(\kappa) = \frac{1}{2\pi}\frac{1}{\kappa^2 + a^2}. \tag{168}$$

A singularity weaker than the cone singularity, with a third derivative discontinuity at a point, is

$$P(r) = r^2\exp(-\sigma r)\ \to \alpha = \frac{3\sigma(2\sigma^2 - 3\kappa^2)}{2\pi\kappa(\sigma^2+\kappa^2)^3\sqrt{1+\sigma^2/\kappa^2}} \sim -\frac{9\sigma}{2\pi\kappa^5} + O(\kappa^{-7}). \tag{169}$$

The product of $K_0(ar)$ with *even* powers of r also yield explicit, rational $\alpha(\kappa)$ as included in the table.

20 Smooth modulations of Gibbs' Phenomenon

The examples above are rather special in that the discontinuous-disk function, for example, is everywhere constant except on the circle of discontinuity. What happens if the amplitude of the jump varies around the circle of discontinuity? What happens if $f(x, y)$ varies radially near the edge of the cliff?

The answer is: very little [103]. Still, it is useful to give an elementary argument using the Fourier Transform in polar coordinates. Suppose that $P(r, \phi) = p_0(r) + \sum_{n=1}^{\infty} p_n(r)\cos(n\phi) + q_n(r)\sin(n\phi)$ where each Fourier coefficient is of the form

$$p_n(r) = \begin{cases} \tilde{p}_n(r), & r \le R \\ 0, & r > R \end{cases}. \tag{170}$$

Then

$$\alpha_n(\kappa) = \frac{(-\mathrm{i})^n}{2\pi} \int_0^\infty J_n(\kappa r)\, p_n(r)\, r\, \mathrm{d}r, \tag{171}$$
$$= \frac{(-\mathrm{i})^n}{2\pi} \int_0^\infty J_n(\kappa r)\, \tilde{p}_n(r)\, r\, \mathrm{d}r - \frac{(-\mathrm{i})^n}{2\pi} \int_R^\infty J_n(\kappa\, r)\, \tilde{p}_n(r)\, r\, \mathrm{d}r.$$

without approximation. There is no loss of generality in assuming that $\tilde{p}_n(r)$ is analytic and decays exponentially fast as $r \to \infty$; since $\tilde{p}_n(r)$ appears in $p_n(r)$ only for $r \le R$, we can extend $\tilde{p}_n(r)$ to large r any way we please without changing the integral of $p_n(r)$ from $r = 0$ to $r = R$. If $\tilde{p}_n(r)$ does not decay for large r, we can apply a C^∞ window as discussed earlier to enforce convergence of the integrals.

By repeated integration-by-parts, one can prove that the infinite integral in (171) decays faster than any finite power of κ as $\kappa \to 0$. Therefore,

$$\alpha_n(\kappa) \sim \frac{-(-\mathrm{i})^n}{2\pi} \int_R^\infty J_n(\kappa r)\, \tilde{p}_n(r)\, r\, \mathrm{d}r + \text{exponentially small in}\, \kappa,\ \ \kappa \gg 1. \tag{172}$$

Now when κ is large, $\kappa R \gg 1$ and therefore we can replace the Bessel functions by their asymptotic approximations:

$$\alpha_n(\kappa) \sim \frac{-(-\mathrm{i})^n}{2\pi} \sqrt{\frac{2}{\pi\kappa}} \int_R^\infty \cos\left(\kappa r - (\pi/2)n - \pi/4\right) \tilde{p}_n(r)\, \sqrt{r}\, \mathrm{d}r, \quad \kappa \gg 1. \tag{173}$$

A single integration-by-parts, integrating the cosine and differentiating the rest of the integrand, gives

$$\alpha_n(\kappa) \sim \frac{(-\mathrm{i})^n}{\sqrt{2}\pi^{3/2}} \frac{1}{\kappa^{3/2}} \cos\left(\kappa r - (\pi/2)n + \pi/4\right) \tilde{p}_n(r)\, \sqrt{r} \Big|_R^\infty$$
$$- \frac{(-\mathrm{i})^n}{\sqrt{2}\pi^{3/2}} \frac{1}{\kappa^{3/2}} \int_R^\infty \cos\left(\kappa r - (\pi/2)n + \pi/4\right) \left\{ \frac{\tilde{p}_n(r)}{2\sqrt{r}} + \frac{\mathrm{d}\tilde{p}_n(r)}{\mathrm{d}r} \sqrt{r} \right\} \mathrm{d}r. \tag{174}$$

One can apply further integrations-by-parts to the remaining integral, adding an additional factor of $1/\kappa$ with each such manipulation, and then one can bound the many-times-modified integral to show that it decays as a high inverse power of κ. However, there is nothing to be done about the boundary term, which gives, for $n = 0, 1, 2, \ldots$,

$$\alpha_n(\kappa) \sim -\frac{(-\mathrm{i})^n}{\sqrt{2}\pi^{3/2}} \frac{1}{\kappa^{3/2}} \cos\left(\kappa R - (\pi/2)n + \pi/4\right) \tilde{p}_n(R)\, \sqrt{R} + O(\kappa^{-5/2}). \tag{175}$$

The same formula applies to the sine coefficients $\beta_n(\kappa)$ with the replacement of $p_n(r)$ by $q_n(r)$.

Thus, if $f(x, y)$ has jumps only along a circle, all the $\alpha_n(\kappa)$ and $\beta_n(\kappa)$ fall as $\kappa^{-3/2}$.

The restriction to a circle of discontinuity is not really a restriction because if the curve of discontinuity $\partial\mathcal{B}$ is *smooth* [and therefore free of corners, unlike a polygon], it can be mapped into the circle by an analytic change of coordinates. We can then apply the same reasoning as before except that the pattern function $P(r, \theta)$ is replaced by the product of the pattern function in the new transformed coordinates (r', θ') multiplied by the Jacobian of the change of coordinate, $J(r', \theta')$. We can expand this product in a Fourier series in polar coordinates as before, and the rest of the derivation goes through unchanged.

This argument cannot be extended to show that $\alpha(\kappa\cos(\phi), \kappa\sin(\phi))$ always decays as $O(\kappa^{-3/2})$ in all directions; this assertion is false for the "square plateau" function. When the domain has *corners*, it cannot be smoothly mapped into a circle and "all, all is changed utterly", to quote Yeats' poem *Easter 1916*.

21 Spiral singularities

When a fluid flow is turbulent, large eddies simultaneously stretch and compress blobs of fluid to create flow patterns of great complexity. Leonardo da Vinci, who coined the word *turbulenza*, sketched the myriad vortices of churning water with the same skill he applied to the *Mona Lisa*. Half a millenium later, turbulence is still as enigmatic as La Gioconda's half-smile.

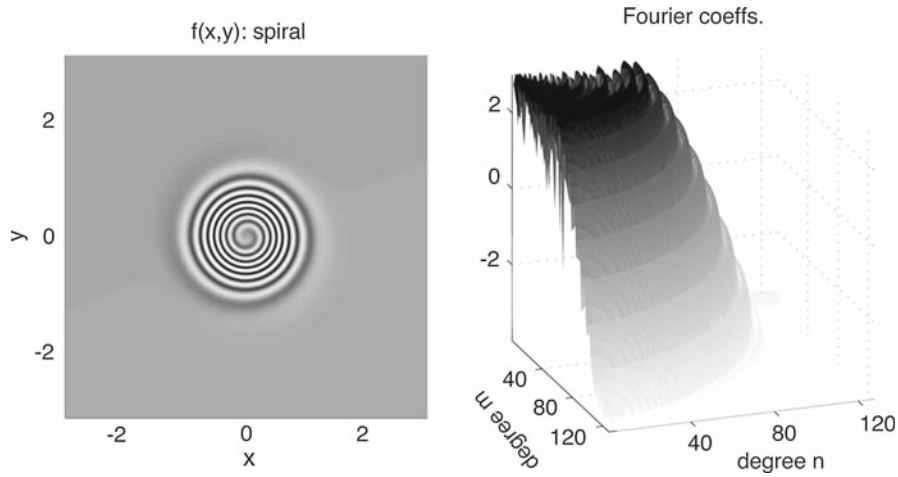

Fig. 14 A typical spiral tracer distribution and its two-dimensional Fourier coefficients

From a pure mathematics viewpoint, there may be no such thing as a "spiral singularity" or indeed any singularity associated with turbulence. Fluids are always viscous, and the same viscosity that makes honey and ketchup sluggish forces the Fourier coefficients to always fall exponentially for very large κ where κ is the magnitude of the wavevector.[1] However, the viscosity is so small for air and water that the "dissipation" range is far beyond the resolution of any present-day computer. In a practical sense, what matters are the intermediate asymptotics, the behavior of Fourier coefficients for those moderately large κ that represent the "inertial range".

For intermediate κ, the energy spectra, which are a plot of the absolute value squared of the Fourier coefficients versus κ, show decay proportional to κ^{-3} in two dimensions and $\kappa^{-5/3}$ in three dimensions. (The atmosphere behaves like two-dimensional turbulence for length scales of $O(1000\,\mathrm{km})$ or more and like three-dimensional turbulence for smaller scales [111]). These imply that from a *practical, numerical* perspective, turbulent flows behave as if they were singular for real values of the coordinates (although these singularities are slightly off the real axis by too small an amount to help turbulence modellers).

"It is natural then to enquire as to what structures in x-space can give rise to such a power-law.", wrote H. K. Moffatt, who argued that the accumulation points of discontinuities associated with spiral structures could create fractional power laws $k^{-\lambda}$ with $1 < \lambda < 2$ [112,113]. Unfortunately, the nature of these singularities is poorly understood, and there is no agreement as to what causes them [112–115].

To give the flavor of this research frontier, we shall retreat from nonlinear dynamics to the easier problem of the advection of a passive tracer by a specified flow, and further simplify by assuming that the flow is a radially-symmetric time-independent vortex with purely tangential flow. If $v(r)$ denotes the tangential velocity, then the exact solution to the two-dimensional tracer advection problem is

$$Q(r,\theta,t) \equiv Q(r,\ \theta - [v(r)/r]\,t, 0). \tag{176}$$

Figure 14 shows a typical case; rewriting $\sin(\theta - [v(r)/r]t)$ as $\sin(\theta)\cos([v(r)/r]t) - \cos(\theta)\sin([v(r)/r]t)$ using a trigonometric identity, the tracer distribution is

$$Q = \exp\left(-\frac{3}{2}\right) r^2 \left\{ r\sin(\theta)\,\cos\left(t\,\exp(-2r^2)\right) - r\cos(\theta)\,\sin\left(t\,\exp(-2r^2)\right)\right\}. \tag{177}$$

For all finite times, the tracer distribution is non-singular, but the numerical challenge grows endlessly as t increases as the turns of the spiral wind tighter and tighter. The Fourier spectrum is flat out to some κ which depends on time

[1] The nonsingularity of viscous turbulent flow, however, is still not rigorously proved [110] and indeed such regularity is one of the Clay Millenium Prizes—$1,000,000 award!

and then falls exponentially fast. For any fixed truncation of the Fourier series, the flat part of the spectrum widens with time until the truncation fails to give any useful accuracy.

Extending this analysis to nonlinear fluid mechanics is very much an unsolved problem.

22 Separation of variables

For centuries, the only method for obtaining *general* solutions to partial differential equations was "separation of variables". We will not repeat the usual textbook *ansatz* because separation of variables is really just a spectral method in which the basis functions in one coordinate are chosen so that the ordinary differential equations in the remaining coordinate are *uncoupled*, and therefore easily solved.

Separation of variables is both beautiful and practical because it yielded the general solution to many linear partial differential equations when number-crunching methods were unavailable. The asymptotic spectral coefficients generated by the methods are rarely discussed, however. This is unfortunate because one flaw of separation of variables is that its spectral series generically converge with only an algebraic rate of convergence. For example, the Poisson equation on the domain $[0, \pi] \otimes [0, \pi]$ with homogeneous Dirichlet boundary conditions can be solved by expanding inhomogeneous term and solution in double sine series:

$$u_{xx} + u_{yy} = -f(x, y), \tag{178}$$

$$f(x, y) = \sum_{m=1}^{\infty} \sum_{n=1}^{\infty} f_{mn} \sin(mx) \sin(ny), \tag{179}$$

$$u(x, y) = \sum_{m=1}^{\infty} \sum_{n=1}^{\infty} \frac{f_{mn}}{m^2 + n^2} \sin(mx) \sin(ny). \tag{180}$$

If $f(x, y)$ is not a periodic function, then its sine coefficients will decrease algebraically and the spectral series will display Gibbs' Phenomenon either for $f(x, y)$ or for a sufficiently high derivative, and these properties are inherited by $u(x, y)$ (though the algebraic order of convergence is increased by two).

A specific and much-studied case is $f(x, y) = 1$, which has the Fourier series

$$f(x, y) = \sum_{m=1}^{\infty} \sum_{n=1}^{\infty} \frac{16}{\pi^2} \frac{1}{(2m-1)(2n-1)} \sin(mx) \sin(my). \tag{181}$$

The series converges at only a first order rate to the two-dimensional sign function:

$$f_{\text{sign}}(x, y) = \begin{cases} 1, & x \in [0, \pi], y \in [0, \pi] \\ -1 & x \in [-\pi, 0], y \in [0, \pi] \\ 1 & x \in [-\pi, 0], y \in [-\pi, 0] \\ -1 & x \in [0, \pi], y \in [-\pi, 0]. \end{cases} \tag{182}$$

The corresponding Poisson solution has only a third order rate of convergence:

$$u(x, y) = \frac{16}{\pi^2} \sum_{m=1}^{\infty} \sum_{n=1}^{\infty} \frac{1}{(2m-1)(2n-1)\left\{(2m-1)^2 + (2n-1)^2\right\}} \sin((2m-1)x) \sin((2n-1)y). \tag{183}$$

A double sine series, which must necessarily be antisymmetric with respect to both $x = 0$ and $y = 0$, i.e., $f(-x, y) = -f(x, y)$ and $f(x, -y) = -f(x, y)$, can converge to the constant one on $[0, \pi] \otimes [0, \pi]$ only by converging to the sign function on the full period box, $[-\pi, \pi] \otimes [-\pi, \pi]$. In general, the forcing and solution to the Poisson equation are *not periodic* and we must expect very bad things (i.e., slow convergence) when solving the problem using a basis of periodic functions. But this is not the whole story.

23 Corner singularities and PDE compatibility conditions

In general, whenever a partial differential equation is posed on a domain with *corners*, whether an elliptic problem in a purely spatial domain, or a hyperbolic or parabolic equation in a space-time domain, the solutions will be *weakly singular in the corners*. This important bit of mathematical folklore is usually omitted from engineering mathematics courses.

In addition, for each species of differential equation, there is a countable infinity of "compatibility conditions" for the initial conditions and inhomogeneous forcing terms which control the asymptotic rate of convergence of the spectral coefficients (or the convergence of any high-order numerical method) by controlling the severity of the corner singularities. Although these compatibility conditions can be derived using functional analysis methods [116–118], one can learn much simply from the spectral series.

These compatibility conditions are not common knowledge even among mathematicians. The Fields Medalist Stephen Smale rediscovered corner singularities on a sabbatical at Michigan [119]. He wrote "One can reasonably ask: to what extent is our main theorem a new result in partial differential equations (apart from the methodology introduced here)? I have not seen it explicitly in the literature and the mathematicians in partial differential equations I've talked to were unaware of it."

For example, the first compatibility condition for the Poisson equation in the square with homogeneous Dirichlet boundary conditions is

$$f(0, y) = f(\pi, y) = f(x, 0) = f(x, \pi) = 0. \tag{184}$$

This removes the incompatibility of approximating a function $f(x, y)$ that does not vanish on all four boundary segments with a double sine series whose terms individually all do vanish at the boundaries. By integration-by-parts, one can show that the double sine series must have at least third order convergence if (184) is satisfied, implying at least fifth-order convergence for the series for the solution $u(x, y)$.

By further two-dimensional integrations-by-parts, one may derive the second-order compatibility conditions, but another argument is more illuminating. One-dimensional integrations-by-parts show that for the series for $f(x, y)$ to converge faster than first order, it is necessary that f_{xx} is zero at both $x = 0$ and $x = \pi$ and similarly f_{yy} must vanish along the other two boundaries, but these conditions are not sufficient for higher order convergence.

Note that Poisson's equation and the vanishing of $f(x, y)$ on all boundary segments imply that, provided that the second derivatives are continuous as necessary for a higher-than-third-order Fourier series, the Laplacian of u must vanish on the boundaries, too. The application of the Laplace operator to the Poisson equation and the introduction of the new unknown $v \equiv \nabla^2 u$ show that $\nabla^2 v = \nabla^2 f$. If v is to converge faster than third order, implying faster than fifth-order convergence for u, then $\nabla^2 f$ must be zero on all sides of the domain. Since one of the second derivatives must, by one-dimensional integration-by-parts, be zero on each boundary line, the other second derivative must vanish, too. Thus, the second-order compatibility condition is

$$f_{xx}(0, y) = f_{xx}(\pi, y) = f_{xx}(x, 0) = f_{xx}(x, \pi) = 0 \text{ and } f_{yy}(0, y) = f_{yy}(\pi, y) = f_{yy}(x, 0) = f_{yy}(x, \pi) = 0. \tag{185}$$

Through similar reasoning, one can derive an infinite number of compatibility conditions for any partial differential equation, linear or nonlinear. Reviews are given in [120,121], but see also [118,122–126].

Chebyshev polynomials are optimum for approximating non-periodic functions, but the rate of convergence in solving the Poisson equation on a domain with corners is still only finite order. The reason is that corner singularities degrade the rate of convergence. For $\nabla^2 u = -1$, it has long been known that, creating a local polar coordinate system centered on one of the corners, the leading singularity is of the form [127]

$$u(x, y) \sim \text{constant } r^2 \log(r) \sin(2\theta) + \text{less singular}, \qquad r \ll 1. \tag{186}$$

Table 2 shows that an otherwise periodic function would have a Fourier series with a fourth order rate of convergence, i. e., $a_{mn} \sim O\left([\sqrt{m^2 + n^2}]^{-4}\right)$. Since the highly anisotropic convergence of the series (183) is only third order, it follows that the biggest flaw with the Fourier series is that it has been applied to a non-periodic problem.

The rate of convergence of the Chebyshev series is, however, controlled by the corner singularities. The Chebyshev series is converted into a Fourier series (more precisely, a double cosine series) by the mappings

$$x = \cos(s), \quad y = \cos(t), \tag{187}$$

so that

$$u(\cos(s), \cos(t)) = \sum_{m=0}^{\infty} \sum_{n=0}^{\infty} a_{mn} \cos(ms) \cos(nt). \tag{188}$$

Near a corner such as $x = 1$, $y = 1$,

$$r \equiv \sqrt{(x-1)^2 + (y-1)^2} \tag{189}$$

$$= \sqrt{(\cos(s)-1)^2 + (\cos(t)-1)^2} \tag{190}$$

$$\approx (1/2)(s^2 + t^2). \tag{191}$$

If we introduce polar coordinates in the $s - t$ plane via

$$s = \rho \cos(\phi), \qquad t = \rho \sin(\phi), \tag{192}$$

then the leading singularity is proportional to

$$\rho^4 \log(\rho). \tag{193}$$

This implies that the Chebyshev coefficients, according to Table 2, should converge at a sixth-order rate as numerically observed by Haidvogel and Zang [128], who noted that the error falls only as fourth order.

The rate of convergence can be improved by either explicitly subtracting the worst singularity from the function that is represented by the Chebyshev series [129] or by using an exponential change of coordinate [47,130–132], which implicitly removes the singularity, too. As stressed before, Darboux's Principle is that singularities control the asymptotic rate of convergence, so spectral coefficients can be accelerated only by removing at least the worst singularities.

The compatibility conditions above arise from the differential equations themselves; corner singularities arise from the geometry of the spatial or space-time domain; there are side conditions that are necessary for rapid convergence of spectral series in the separation of variables.

These basis-dependent side conditions deserve a little more discussion because they arise also for partial differential equations on domains that lack corners. For example, when the Poisson equation in the unit disk with homogeneous Dirichlet boundary conditions is solved by the method of separation of variables in polar coordinates, the series of Bessel functions in the radial coordinate has a finite algebraic order of convergence which is controlled by an infinite set of side conditions on the inhomogeneous term in the differential equation, $f(r, \theta)$ [120]. In contrast, a Chebyshev series in radius has an *exponential* rate of convergence if $f(r, \theta)$ is analytic everywhere on the disk including its boundaries. The disadvantage of the Chebyshev series, just as for the Poisson equation on a rectangle, is that the set of ordinary differential in radius are *coupled* whereas these become uncoupled ("separated", in the jargon of the separation of variables method) if the slow-converging Bessel series is used instead.

In summary, the geometry, the differential equation, and the basis all can degrade the rate of convergence of a spectral series. The choice of basis is the only one of these factors that is user-choosable, but an exponential rate of convergence is often purchased at the price of abandoning the simplicity of the method of separation of variables. When there are corner singularities, it is not possible to obtain an exponential rate of convergence from *any* choice of basis.

24 Summary and open problems

Much is known about the asymptotic behavior of spectral coefficients. In particular, each singularity of $f(x)$ contributes a term to the coefficient a_n; the behavior as $n \to \infty$ is dominated by the singularity whose contribution decays

most slowly with degree n. The contributions of poles and branch points can be calculated using the usual complex variable tools of residues (for poles) and keyhole shaped contours (for branch points). The method of steepest descent has been applied often to assess the effects of singularities such that the function is infinitely differentiable even at the singular point; such C^∞ singularities are the rule rather than the exception for expansions on an unbounded interval. The conditions for the coefficients to decay exponentially fast and a bound on the rate of convergence when these conditions are violated can be obtained by repeated integration-by-parts, which often also yields an asymptotic approximation of a_n in inverse powers of n.

However, there are many open problems including the following:

1. If $f(x)$ is a C^∞ function of Gevrey order G and r is the exponential index of (subgeometric) convergence, are there functions for which $r < 2/(G+2)$?
2. A careful proof of Darboux's Principle, generalizing his theorem for power series to other species of spectral expansions.
3. Approximations for the contributions of complicated singularities such as cosines-of-logarithms.
4. Asymptotic spectral theory for prolate spheroidal wavefunctions and spherical harmonics, beyond rudimentary integration-by-parts arguments.
5. Asymptotic approximations for functions with singularities of fractal structure and natural boundaries in the complex plane.

Acknowledgements This work was supported by the National Science Foundation through grant OCE 0451951. I thank Scott McCue, the editor of this special issue, for his invitation to contribute and his editing. I thank Mark A. Pinsky and Michael Taylor for helpful correspondence.

References

1. Boyd JP (2001) Chebyshev and Fourier spectral methods, 2nd edn. Dover, Mineola
2. Lyness JN (1971) Adjusted forms of the Fourier Coefficient Asymptotic Expansion. Math Comput 25:87–104
3. Lyness JN (1984) The calculation of trigonometric Fourier coefficients. J Comput Phys 54:57–73
4. Davis PJ (1959) On the numerical integration of periodic analytic functions. In: Langer RE (ed) Numerical approximation. University of Wisconsin Press, Madison, pp 45–59
5. Boyd JP (1998) Weakly nonlocal solitary waves and beyond-all-orders asymptotics: generalized solitons and hyperasymptotic perturbation theory, volume 442 of Mathematics and its applications. Kluwer, Amsterdam
6. Boyd JP (1999) The devil's invention: asymptotics, superasymptotics and hyperasymptotics. Acta Applicandae 56:1–98
7. Segur H, Tanveer S Levine H (eds) (1991) Asymptotics beyond all orders. Plenum, New York, p 389
8. Dingle RB (1973) Asymptotic expansions: their derivation and interpretation. Academic, New York
9. Arteca GA, Fernandez FM, Castro EA (1990) Large order perturbation theory and summation methods in quantum mechanics. Springer, New York
10. Jones DS (1997) Introduction to asymptotics: a treatment using nonstandard analysis. World Scientific, Singapore
11. Kowalenko V, Glasser ML, Taucher T, Frankel NE (1995) Generalised Euler-Jacobi inversion formula and asymptotics beyond all orders, volume 214 of London Mathematical Society Lecture Note Series. Cambridge University Press, Cambridge
12. Le Guillou JC, Zinn-Justin J (eds) (1990) Large-order behaviour of perturbation theory. North-Holland, Amsterdam
13. Lombardi E (2000) Oscillatory integrals and phenomenon beyond all algebraic orders, volume 1741 of Lecture Notes in Mathematics. Springer, New York
14. Paris RB, Kaminski D (2001) Asymptotics and Mellin-Barnes integrals. Cambridge University Press, Cambridge
15. Sternin BY, Shatalov VE (1996) Borel-Laplace transform and asymptotic theory: introduction to resurgent analysis. CRC Press, New York
16. Wong R (ed) (1990) Asymptotic and computational analysis. Marcel Dekker, New York
17. Balser W (1999) Formal power series and linear systems of meromorphic ordinary differential equations. Springer, New York
18. Grosch CE, Orszag SA (1977) Numerical solution of problems in unbounded regions: coordinate transforms. J Comput Phys 25:273–296
19. Boyd JP (1982) The optimization of convergence for Chebyshev polynomial methods in an unbounded domain. J Comput Phys 45:43–79
20. Boyd JP (1987) Spectral methods using rational basis functions on an infinite interval. J Comput Phys 69:112–142
21. Boyd JP (1990) The orthogonal rational functions of Higgins and Christov and Chebyshev polynomials. J Approx Theor 61: 98–103

22. Christov CI (1982) A complete orthonormal system in $L^2(-\infty, \infty)$ space. SIAM Appl Math 42:1337–1344
23. Christov CI, Bekyarov KL (1990) A Fourier-series method for solving soliton problems. SIAM J Sci Stat Comput 11:631–647
24. Bekyarov KL, Christov CI (1991) Fourier-Galerkin numerical technique for solitary waves of fifth order Korteweg-DeVries equation. Chaos Solitons Fract 5:423–430
25. Christou MA, Christov CI (2002) Fourier-Galerkin method for interacting localized waves. Neural Parallel Sci Comput 10: 431–446
26. Christou MA, Christov CI (2002) Fourier-Galerkin method for localized solutions of equations with cubic nonlinearity. J Comput Anal Appl 4:63–77
27. Christou MA, Christov CI (2005) Localized waves for the regularized long wave equation via a Galerkin spectral method. Math Comput Simul 69:257–258
28. Christou MA, Christov CI (2005) Fourier-Galerkin method for 2D solitons of Boussinesq equation. Math Comput Simul 74:82–92
29. Boyd JP (1987) Orthogonal rational functions on a semi-infinite interval. J Comput Phys 70:63–88
30. Boyd JP, Rangan C, Buchsbaum PH (2003) Pseudospectral methods on a semi-infinite interval with application to the hydrogen atom: a comparison of the mapped Fourier-sine method with Laguerre series and rational Chebyshev expansion. J Comput Phys 188:56–74
31. Boyd JP (1984) The asymptotic coefficients of Hermite series. J Comput Phys 54:382–410
32. Darboux MG (1878) Mémoire sur l'approximation des fonctions de très-grands nombres, et sur une classe étendue de développements en série. Math Pures Appl 4:5–56
33. Darboux MG (1878) Mémoire sur l'approximation des fonctions de très-grands nombres, et sur une classe étendue de développements en série. Math Pures Appl 4:377–416
34. Hunter C, Guerrieri B (1980) Deducing the properties of singularities of functions from their Taylor series coefficients. SIAM J Appl Math 39:248–263
35. Hunter C (1987) Oscillations in the coefficients of power series. SIAM J Appl Math 4:483–497
36. Delves LM, Mead KO (1971) On the convergence rates of variational methods I Asymptotically diagonal systems. Math Comput 25:699–716
37. Mead KO, Delves LM (1973) On the convergence rate of generalized Fourier expansions. J Inst Math Appl 12:247–259
38. Schwartz C (1963) Estimating convergence rates of variational calculations. Meth Comput Phys 2:241–266
39. Sulem C, Sulem PL, Frisch H (1983) Tracing complex singularities with spectral methods. J Comput Phys 50:138–161
40. Mhaskar HN, Prestin J (2000) On detection of singularities of a periodic function. Adv Comput Math 12:95–131
41. Weideman JAC (2003) Computing the dynamics of complex singularities in nonlinear PDEs. SIAM J Appl Dyn Syst 2:171–186
42. Pauls W, Matsumoto T, Frisch U, Bec J (2006) Nature of complex singularities for the 2d Euler equation. Phys D 219:40–59
43. Della Rocca G, Lombardo MC, Sammartino M, Sciacca V (2006) Singularity tracking for Camassa-Holm and Prandtl's equations. Appl Numer Math 56:1108–1122
44. Cichowlas C, Brachet ME (2005) Evolution of complex singularities in Kida-Pelz and Taylor-Green inviscid flows. Fluid Dyn Res 36:239–248
45. Scraton RE (1970) A method for improving the convergence of Chebyshev series. Comput J 13:202–203
46. Tee T, Trefethen LN (2006) A rational spectral collocation method with adaptively transformed Chebyshev grid points. SIAM J Sci Comput 28:1798–1811
47. Boyd JP (1986) Polynomial series versus sinc expansions for functions with corner or endpoint singularities. J Comput Phys 64:266–269
48. Boyd JP (1985) Complex coordinate methods for hydrodynamic instabilities and Sturm-Liouville problems with an interior singularity. J Comput Phys 57:454–471
49. Boyd JP (2004) Prolate elements: prolate spheroidal wavefunctions as an alternative to Chebyshev and Legendre polynomials for spectral and pseudospectral algorithms. J Comput Phys 199:688–716
50. Barray DA, Parlange JY, Li L, Prommer H, Cunningham CJ, Stagnitti E (2000) Analytical approximations for real values of the Lambert W-function. Math Comput Simul 53:95–103
51. Davis PJ (1975) Interpolation and approximation. Dover, New York
52. Bain M (1978) On the uniform convergence of generalized Fourier series. J Inst Math Appl 21:379–386
53. Bain M, Delves LM (1977) Convergence rates of expansions in Jacobi polynomials. Numer Math 27:219–225
54. Luke YL (1969) The special functions and their approximations, vol I & II. Academic Press, New York
55. Luke YL Mathematical functions and their approximations. Academic Press, New York
56. Németh GN (1992) Mathematical approximation of special functions: ten papers on Chebyshev expansions. Nova Science Publishers, New York
57. Snyder MA (1966) Chebyshev methods in numerical approximation. Prentice-Hall, Englewood Cliffs
58. Elliott D (1960) The expansion of functions in ultraspherical polynomials. J Aust Math Soc 1:428–438
59. Elliott D (1964) The evaluation and estimation of the coefficients in the Chebyshev series expansion of a function. Math Comput 18:274–284
60. Elliott D (1965) Truncation errors in two Chebyshev series approximations. Math Comput 19:234–248
61. Elliott D, Szekeres G (1965) Some estimates of the coefficients in the Chebyshev expansion of a function. Math Comput 19:25–32
62. Elliott D, Tuan PD (1974) Asymptotic coefficients of Fourier coefficients. SIAM J Math Anal 5:1–10
63. Tuan PD, Elliott D (1972) Coefficients in series expansions for certain classes of functions. Math Comput 26:213–232

64. Wimp J (1961) Polynomial approximations to integral transforms. Math Comput 15:174–178
65. Wimp J (1962) Polynomial expansions of Bessel functions and some associated functions. Math Comput 16:446–458
66. Miller PD (2006) Applied asymptotic analysis. American Mathematical Society Providence, Rhode Island
67. Bender CM, Orszag SA (1978) Advanced mathematical methods for scientists and engineers. McGraw-Hill, New York, 594 pp
68. Boyd JP (2002) A comparison of numerical algorithms for Fourier extension of the first, second and third Kinds. J Comput Phys 178:118–160
69. Boyd JP (2005) Fourier embedded domain methods: extending a function defined on an irregular region to a rectangle so that the extension is spatially periodic and C^∞. Appl Math Comput 161:591–597
70. Boyd JP (2006) Asymptotic Fourier coefficients for a C^∞ bell (Smoothed-"Top-Hat" Function) and the Fourier extension problem. J Sci Comput 29:1–24
71. Miller GF (1966) On the convergence of Chebyshev series for functions possessing a singularity in the range of representation. SIAM J Numer Anal 3:390–409
72. Sibuya Y (1990) Gevrey property of formal solutions in a parameter. In: Wong R (ed) Asymptotic and computational analysis. Marcel Dekker, New York, pp 393–401
73. Boyd JP (1981) The rate of convergence of Chebyshev polynomials for functions which have asymptotic power series about one endpoint. Math Comput 37:189–196
74. Boyd JP (1982) A Chebyshev polynomial rate-of-convergence theorem for Stieltjes functions. Math Comput 39:201–206
75. Boyd JP (1994) Asymptotic Chebyshev coefficients for two functions with very rapidly or very slowly divergent power series about one endpoint. Appl Math Lett 9:11–15
76. Berry MV (1991) Stokes phenomenon for superfactorial asymptotic series. Proc R Soc Lond A 435:437–444
77. Boyd JP (1994) The rate of convergence of Fourier coefficients for entire functions of infinite order with application to the Weideman-Cloot sinh-mapping for pseudospectral computations on an infinite interval. J Comput Phys 110:360–372
78. Weideman JAC (1994) Computation of the complex error function. SIAM J Numer Anal 31:1497–1518. Errata: (1995) 32:330–331]
79. Watson GN (1910) The harmonic functions associated with the parabolic cylinder. Proc Lond Math Soc 8:393–421
80. Hille E (1940) Contributions to the theory of Hermitian series II. The representation problem. Trans Am Math Soc 47:80–94
81. Hille E (1939) Contributions to the theory of Hermitian series. Duke Math J 5:875–936
82. Xiao H, Rokhlin V, Yarvin N (2001) Prolate spheroidal wavefunctions, quadrature and interpolation. Inverse Prob 17:805–838
83. Boyd JP (2003) Approximation of an analytic function on a finite real interval by a bandlimited function and conjectures on properties of prolate spheroidal functions. Appl Comput Harmonic Anal 15:168–176
84. Boyd JP (2005) Computation of grid points, quadrature weights and derivatives for spectral element methods using prolate spheroidal wave functions – prolate elements. ACM Trans Math Softw 31:149–165
85. Kovali N, Lin W, Carin L (2005) Pseudospectral method based on prolate spheroidal wave functions for frequency-domain electromagnetic simulations. IEEE Trans Antennas Propag 53:3990–4000
86. Kovvali N, Lin W, Zhao Z, Couchman L, Carin L (2006) Rapid prolate pseudospectral differentiation and interpolation with the fast multipole method. SIAM J Sci Comput 28:485–497
87. Lin W, Kovvali N, Carin L (2006) Pseudospectral method based on prolate spheroidal wave functions for semiconductor nanodevice simulation. Comput Phys Commun 175:78–85
88. Boyd JP (1999) The Blasius function in the complex plane. J Exp Math 8:381–394
89. Chang YF, Greene JM, Tabor M, Weiss J (1983) The analytic structure of dynamical systems and self-similar natural boundaries. Physica D 8:183-
90. Chang YF, Tabor M, Weiss J (1983) Analytic structure of the Henon-Heiles Hamiltonian in integrable and nonintegrable regimes. J Math Phys 23:531
91. Levine G, Fournier JD, Tabor M (1988) Singularity clustering in the duffing oscillator. J Phys A 21 (1988) 33–
92. Takaoka N (1989) Pole distribution and steady pulse solution of the fifth order Korteweg-deVries equation. J Phys Soc JPn 58:73–81, Addendum, vol 58, p 3028
93. Huang NN, Strichartz RS (2001) Sampling theory for functions with fractal spectrum. Exp Math 10:619–638
94. Igari S (1968) Lectures on Fourier series of several variables. Department of Mathematics, University of Wisconsin, Madison
95. Baszenski G, Delvos F (1983) Accelerating the rate of convergence of bivariate Fourier expansions. In: Chou CK et al (eds) Approximation theory IV. Academic Press, New York, pp 335–340
96. Bochner S, Martin WT (1948) Several complex variables. Princeton University Press, Princeton
97. Gray A, Pinsky M (1992) Gibbs phenomenon for Fourier-Bessel series. Exp Math 1:313–316
98. Gray A, Pinsky M (1993) Gibbs phenomenon for Fourier-Bessel series. Expositiones Mathematicae 11:123–135
99. Brandolini L, Colzani L, Iosevich A, Travaglini G (2002) The rate of convergence of Fourier expansions in the plane: a geometric viewpoint. Mathematische Zeitschrift 242:709–724
100. Brandolini L, Iosevich A, Travaglini G (2003) Planar convex bodies, Fourier Transform, lattice points and irregularities of distribution. Trans Am Math Soc 355:3513–3535
101. Helmberg G (1999) A corner point Gibbs phenomenon for Fourier series in two dimensions. J Approx Theor 100:1–43
102. Helmberg G (2002) Localization of a corner point Gibbs phenomenon for Fourier series in two dimensions. J Fourier Anal Appl 8:29–41
103. Helmberg G (2003) An edge point Gibbs phenomenon for Fourier series in two dimensions. Monatshefte fur Mathematik 139: 221–225

104. Taylor M (2001) Eigenfunction expansions and the Pinsky phenomenon on compact manifolds. J Fourier Anal Appl 7507–522
105. Ikromov IA (1995) Estimates for the Fourier transform of the indicator function for nonconvex domains. Funct Anal Appl 29: 161–167
106. Pinsky MA, Stanton NK, Trapa PE (1993) Fourier series of radial functions in several variables. J Funct Anal 116:111–132
107. Bain M, Delves LM, Mead KO (1978) On the rate of convergence of multidimensional orthogonal expansions. Inst Math Appl 21:379–386
108. Podkorytov AN (1991) On the asymptotics of the Fourier transform on a convex curve. Vestn Leningrad Univ Math 24:57–65
109. Abramowitz M, Stegun IA (1972) Handbook of mathematical functions. Dover, New York
110. Kerr RM (2005) Vortex collapse and turbulence. Fluid Dyn Res 36:249–260
111. Lindborg E (1999) Can the atmospheric kinetic energy spectrum be explained by two-dimensional turbulence. J Fluid Mech 388:259–288
112. Moffatt HK (1984) Simple topological aspects of turbulent vorticity dynamics. In: Tatsumi T (ed) Turbulence and chaotic phenomena in fluids. Elsevier, Amsterdam, pp 223–230
113. Moffatt HK (1991) Spiral structures in turbulent flow. In: New approaches and concepts in turbulence, Monte Verita. Birkhauser, Basel, pp 121–129
114. Gilbert AD (1988) Spiral structures and spectra in two-dimensional turbulence. J Fluid Mech 193:475–497
115. Farge M, Holschneider M (1991) Interpretation of two-dimensional turbulence energy spectrum in terms of quasi-singularity in some vortex cores. Europhys Lett 15:737–743
116. Rauch JB, Massey FJ (1974) Differentiability of solutions to hyperbolic initial-boundary value problems. Trans Am Math Soc 189:303–318
117. Sakamoto R (1978) Hyperbolic boundary value problems. Cambridge University Press, Cambridge (1982), 204 pp; first published in Japanese in 1978
118. Ladyzenskaja O (1952) On the convergence of Fourier series defining a solution of a mixed problem for hyperbolic equations. Doklady Akad Nauk SSSR 85:481–484
119. Smale S (1980) Smooth solutions of the heat and diffusion equations. Comment Math Helvetici 55:1–12
120. Boyd JP, Flyer N (1999) Compatibility conditions for time-dependent partial differential equations and the the rate of convergence of Chebyshev and Fourier spectral methods. Comput Meth Appl Mech Eng 175:281–309. Errata: in Eq(22), the square root should be in front of the integral, not in the exponential
121. Témam R (2006) Suitable initial conditions. J Comput Phys 218:443–450
122. Flyer N, Swarztrauber PN (2002) The convergence of spectral and finite difference methods for initial-boundary value problems. SIAM J Sci Comput 23:1731–1751
123. Flyer N, Fornberg B (2003) On the nature of initial-boundary value solutions for dispersive equations. J Comput Phys 64:546–564
124. Deville M, Kleiser L, Montigny-Rannou F (1984) Pressure and time treatment for Chebyshev spectral solution of a Stokes problem. Int J Numer Meth Fluids 4:1149–1163
125. Moffatt HK (1964) Viscous and resistive eddies near a sharp corner. J Fluid Mech 18:1–18
126. Témam R (1982) Behaviour at time $t = 0$ of the solutions of semi-linear evolution equations. J Diff Eqns 43:73–92
127. Boyd JP (1985) An analytical and numerical study of the two-dimensional Bratu equation. J Sci Comput 1:183–206
128. Haidvogel DB, Zang TA (1979) The accurate solution of Poisson's equation by expansion in Chebyshev polynomials. J Comput Phys 30:167–180
129. Schultz WW, Lee NY, Boyd JP (1989) Chebyshev pseudospectral method of viscous flows with corner singularities. J Sci Comput 4:1–24
130. Boyd JP (2005) A spectrally-accurate quadrature for resolving the logarithmic endpoint singularities of the Chandrasekhar H-function. J Quant Spectrosc Radiat Transfer 94:467–475
131. Boyd JP (2005) A Chebyshev/Rational Chebyshev spectral method for the Helmholtz equation in a sector on the surface of a sphere: defeating corner singularities. J Comput Phys 206:302–310
132. Boyd JP (1989) The asymptotic Chebyshev coefficients for functions with logarithmic endpoint singularities. Appl Math Comput 29:49–67